International Journal of Plant Sciences

# THE ARCHAEOPTERID FORESTS OF WYOMING: FLORA AND DEPOSITIONAL ENVIRONMENT OF THE UPPER DEVONIAN (LOWER FRASNIAN) MAYWOOD FORMATION

--Manuscript Draft--

| | |
|---|---|
| **Article Type:** | Special issue - Francis Hueber Tribute |
| **Manuscript Number:** | |
| **Full Title:** | THE ARCHAEOPTERID FORESTS OF WYOMING: FLORA AND DEPOSITIONAL ENVIRONMENT OF THE UPPER DEVONIAN (LOWER FRASNIAN) MAYWOOD FORMATION |
| **Corresponding Author:** | Alexandru M.F. Tomescu<br>Humboldt State Universirty<br>Arcata, California UNITED STATES |
| **Corresponding Author's Institution:** | Humboldt State Universirty |
| **Other Authors:** | John Marshall, PhD |
| | Peter Holterhoff, PhD |
| | Samar El-Abdallah |
| | Kelly Matsunaga, PhD |
| | Allison Bronson, PhD |
| **Abstract:** | Premise of research. The flora of the Maywood Formation, one of only three Devonian floras previously recognized in western North America, is known only from a brief report focused on stratigraphy and has never been characterized in more detail. A detailed assessment of this flora and associated fossils has implications for the age and depositional environments of the Maywood Formation, and for Devonian plant biogeography.<br>Methodology. Field work at the Cottonwood Canyon (Wyoming) exposure of the Maywood formation produced a measured section characterizing the sedimentology of the unit and samples that we analyzed for palynomorph, macrofloral, and faunal content using standard methods.<br>Pivotal results. The palynological assemblage is dominated by archaeopterid progymnosperm spores, lacks unequivocally marine components, indicates low burial depth and temperature (c. 53°C) of the unit, and supports an early Frasnian age. Plant macro- and mesofossils including charcoal, adpressions, sporangia, and spore packages reflect a vegetation with quasi-monodominant archaeopterids but also including the parent plant of the seed-megaspore Spermasporites (for which the Cottonwood Canyon occurrence represents a geographic range extension). Scales indicate the presence of sarcopterygian and tetrapodomorph fishes. Sedimentary facies, palynofacies, and plant macrofossil taphonomy are consistent with a lagoon or lake margin environment on a carbonate platform, disconnected from the open marine realm.<br>Conclusions. The arid carbonate platform of the western margin of early Frasnian Laurentia hosted a fire-prone vegetation cover heavily dominated by archaeopterid progymnosperms. The Maywood Formation preserves fossil assemblages reflecting this vegetation at Cottonwood Canyon (Wyoming), in lagoonal or lacustrine deposits that also host microconchid tubeworms and fish. The parent plant of the seed-megaspore Spermasporites, present in this vegetation, was widely distributed all across Euramerica. |
| **Suggested Reviewers:** | Reed Wicander, PhD<br>The University of Queensland<br>r.wicander@uq.edu.au<br>Devonian palynology specialist |
| | Geoffrey Playford, PhD<br>The University of Queensland<br>g.playford@uq.edu.au |

| | |
|---|---|
| | Devonian palynology specialist |
| | Charles Wellman, PhD<br>The University of Sheffield<br>c.wellman@Sheffield.ac.uk<br>Devonian palynology specialist |
| | Chris Berry, PhD<br>Cardiff University<br>Berrycm@cardiff.ac.uk<br>Devonian paleobotany specialist |
| | Brigitte Meyer-Berthaud<br>Universite de Montpellier<br>meyerberthaud@cirad.fr<br>Devonian paleobotany specialist |
| | Anne-Laure Decombeix, PhD<br>Universite de Montpellier<br>anne-laure.decombeix@cirad.fr<br>Devonian paleobotany specialist |
| **Opposed Reviewers:** | |
| **Author Comments:** | We suggest Dr. Kathleen Pigg for handling this manuscript, since two of the authors (Tomescu and Matsunaga) are the editors of the Hueber special issue. |

Cover Letter

HUMBOLDT STATE UNIVERSITY
Department of Biological Sciences

January 13, 2022

The Editor-in-Chief
*International Journal of Plant Sciences*

Dear Editor,

Please fined appended a manuscript titled “The archaeopterid forests of Wyoming: flora and depositional environment of the Upper Devonian (lower Frasnian) Maywood Formation” that my co-authors and I would like to be considered for publication in the Francis Hueber Tribute special issue of the International Journal of Plant Sciences.

Because both myself and one of my co-authors, Dr. Kelly Matsunaga, are editors of the Hueber special issue, I suggest that this manuscript be handled by Dr. Kathleen Pigg.

Sincerely,

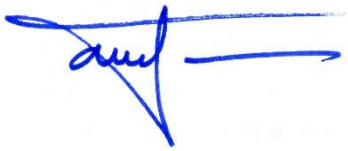

Alexandru M.F. Tomescu
Professor of Botany

1 Harpst Street • Arcata, California 95521-8299 • 707.826.3245 • fax 707.826.3201 • www.humboldt.edu

# THE ARCHAEOPTERID FORESTS OF WYOMING: FLORA AND DEPOSITIONAL ENVIRONMENT OF THE UPPER DEVONIAN (LOWER FRASNIAN) MAYWOOD FORMATION

John E.A. Marshall[1,5], Peter F. Holterhoff[2,5], Samar R. El-Abdallah[3], Kelly K.S. Matsunaga[4], Allison W. Bronson[3], Alexandru M.F. Tomescu[3,5]

[1] School of Ocean and Earth Science, University of Southampton, National Oceanography Centre, European Way, Southampton SO14 3ZH

[2] Hess Corporation, 1501 McKinney Street, Houston, TX 77010

[3] Department of Biological Sciences, Humboldt State University, Arcata, California 95521, USA

[4] Department of Ecology and Evolutionary Biology and Biodiversity Institute, University of Kansas, Lawrence, Kansas 66045, USA

[5] Authors for correspondence; email: jeam@soton.ac.uk, pholterhoff@hess.com, mihai@humboldt.edu



Keywords: charcoal, Devonian, fossil, progymnosperm, palynology, Wyoming

**ABSTRACT**

*Premise of research*. The flora of the Maywood Formation, one of only three Devonian floras previously recognized in western North America, is known only from a brief report focused on stratigraphy and has never been characterized in more detail. A detailed assessment of this flora and associated fossils has implications for the age and depositional environments of the Maywood Formation, and for Devonian plant biogeography.

*Methodology*. Field work at the Cottonwood Canyon (Wyoming) exposure of the Maywood formation produced a measured section characterizing the sedimentology of the unit and samples that we analyzed for palynomorph, macrofloral, and faunal content using standard methods.

*Pivotal results*. The palynological assemblage is dominated by archaeopterid progymnosperm spores, lacks unequivocally marine components, indicates low burial depth and temperature (c. 53°C) of the unit, and supports an early Frasnian age. Plant macro- and mesofossils including charcoal, adpressions, sporangia, and spore packages reflect a vegetation with quasi-monodominant archaeopterids but also including the parent plant of the seed-megaspore *Spermasporites* (for which the Cottonwood Canyon occurrence represents a geographic range extension). Scales indicate the presence of sarcopterygian and tetrapodomorph fishes. Sedimentary facies, palynofacies, and plant macrofossil taphonomy are consistent with a lagoon or lake margin environment on a carbonate platform, disconnected from the open marine realm.

*Conclusions*. The arid carbonate platform of the western margin of early Frasnian Laurentia hosted a fire-prone vegetation cover heavily dominated by archaeopterid progymnosperms. The Maywood Formation preserves fossil assemblages reflecting this vegetation at Cottonwood Canyon (Wyoming), in lagoonal or lacustrine deposits that also host microconchid tubeworms and fish. The parent plant of the seed-megaspore *Spermasporites*, present in this vegetation, was widely distributed all across Euramerica.

## Introduction

Central to any understanding of the Devonian Earth System and the Mid and Late Devonian extinction events is afforestation. What plant groups were involved, how they were distributed around the globe and when this happened, are key questions that require answers. Plant morphology remained relatively simple for much of the Silurian and dramatic increases in complexity and canopy height only really started in the late Early Devonian. Forests of the cladoxylopsid *Calamophyton* are known from the Eifelian of Europe (Giesen and Berry 2013) and are extensive, formed by another cladoxylopsid – *Eospermatopteris* –, in the Givetian of North America (Stein et al. 2007). In the Eifelian of Euramerica, the spore evidence is for vegetation dominated by an aneurophytalean progymnosperm (*Tetraxlyopteris* with *in situ Rhabdosporites langii*) and a lycopsid (represented by *Ancyrospora*) (Marshall 1996). Hammond and Berry (2005) have suggested that these would have grown more as thickets than forests, so the tetraxylopterids could support each other. The first of the tree-sized archaeopteridalean progymnosperm forests appear in the early Givetian, as *Archaeopteris-Eospermatopteris* mixed forests (Stein et al. 2012; Stein et al. 2020) in eastern North America. While these localities were broadly located in the southern hemisphere arid zone, the eastern North American–Appalachian localities were impacted by orographic effects from the Acadian Mountains, which created a humid region that reached across the southern trades during the Mid and Late Devonian. To the north, in the paleo-equatorial zone, there were lycopod forests of *Protolepidodendropsis* that also included *Archaeopteris* (Berry and Marshall 2015). Here, these lycopod forests formed coal bearing wetlands (Marshall et al. 2019) in the Givetian and Frasnian. Among all these different canopy-forming plants, *Archaeopteris* was probably the more prominent ecosystem engineer, with its deeper and laterally more extensive rooting systems (Algeo et al. 2001; Stein et al. 2020). It is possible that the distribution of these forests was influenced by Devonian extinction events, in particular the Taghanic Event that ~~stripped out~~ eliminated much of the non-*Archaeopteris* diversity.

Much of our knowledge of Devonian forests comes from the better studied areas of Euramerica. Yet, toward its western margin, the Old Red Sandstone continent continued as an extensive carbonate platform across the North American Midwest. The vegetation cover of this area is very sparsely documented because carbonate sequences tend to preserve very poor palynological and paleobotanical records. Only three floras – none of which has been extensively characterized – have been reported from Devonian deposits in western North America: the Martin Formation flora of Arizona, the Chilliwack Group flora of Washington State, and the Maywood Formation flora of Wyoming. While the ages of these floras were not precisely constrained previously, the first two are thought to be Early to Mid

Devonian (Teichert and Schopf 1958; Canright 1970; Benca et al. 2014). The flora of the Maywood Formation (also referred to as the Souris River Formation) was first reported by Sandberg (1963) from an exposure in Cottonwood Canyon (Wyoming). Based on the fossil plant and fish content, Sandberg assigned a Late Devonian (Frasnian) age to the Maywood Formation, which he viewed as representing brackish to nearly freshwater deposits of an estuary. Since Sandberg's 1963 report, the fossil assemblages of Maywood Formation at Cottonwood Canyon have remained unexplored until very recently, when Zaton et al. (2021) characterized the microconchid tubeworm fauna and assigned a late Mid Devonian (Givetian) age based on the palynomorph content. Here, we address the age of the Maywood Formation in the Cottonwood Canyon exposure, and report on the vegetation and depositional environments of the western edge of the Laurentian carbonate platform as reflected in the palynoflora and macroflora of this rock unit.

## Material and Methods

### *Regional Geology and Stratigraphic Framework*

The study section in Cottonwood Canyon is located on the northwestern flank of the Bighorn Mountains, approximately 27 kilometers east of Lovell, Big Horn County, Wyoming (44° 52' 14.08" N, 108° 3' 26.21" W; fig. 1). The entire exposed Paleozoic section at the study site dips strongly to the west over a blind Laramide (Paleogene) thrust.

The Middle Paleozoic succession of the Bighorn Mountains of north-central Wyoming was deposited on a northward extension of the Transcontinental Arch, which reached as far north as the Central Montana Uplift, effectively separating the Williston Basin of eastern Montana and North Dakota from basins to the west in Utah, Idaho, and western Montana (Sandberg 1961a; Johnson et al. 1988; Hoffman 2020). The Cottonwood Canyon section discussed in this paper is located in the western region of this long-lived positive feature. Thus, the Ordovician through Devonian succession exposed in Cottonwood Canyon is characterized by thin and/or patchy packages bounded by large unconformities representing non-deposition and erosion (fig. 2).

The Upper Ordovician Bighorn Dolomite and Upper Devonian Jefferson Formation are confidently mapped in continuity across the northern Wyoming and Montana region. However, the Lower Devonian Beartooth Butte Formation and the Upper Devonian Maywood Formation are isolated occurrences in Cottonwood Canyon and cannot be mapped continuously to the basins to the north. The stratal unit here interpreted as Maywood Formation has been particularly problematic to diagnose. This unit was regarded as Souris River Formation (?) by Sandberg (1963) and then definitively called Souris

River Formation by Sandberg (1967). The Souris River is a unit named for a sub-surface succession of mixed carbonates, siliciclastics, and evaporites in the Williston Basin, where it lies beneath the Duperow Formation (= Jefferson Formation of northern Wyoming and western Montana) (Sandberg 1961a). The Souris River is dominantly early Late Devonian (Early Frasnian) in age but may be as old as late Mid Devonian (Givetian) in the central part of the basin (Sandberg 1961a). Sandberg's (1963) original attribution of the Cottonwood Canyon strata to the Souris River was based on vertebrates (fish) and palynology data indicating an early Frasnian age for the deposit, thus implying they were coeval with the Souris River Formation. However, it should be noted that the Cottonwood Canyon section is approximately 180 kilometers from the nearest recognized Souris River Formation occurrence in the Williston Basin region (Sandberg 1961a) and no physical correlation can be established between the two.

Sandberg et al. (1982) subsequently referred the Cottonwood Canyon section to the Maywood Formation, although earlier workers had already noted the close relationship between the Maywood Formation of western Montana and the section exposed at Cottonwood Canyon, Wyoming (Mikesh 1965; Benson 1966). Sandberg and McMannis (1964) made direct comparisons between the fish and plant fossils of a Maywood channel-form deposit in the Gallatin Mountains of southwestern Montana to the Souris River (?) section in Cottonwood Canyon, as reported by Sandberg (1963). The Maywood has been mapped in continuity with the Souris River across northern Montana, thus the units are considered lithostratigraphic equivalents (Hoffman 2020).

The Maywood Formation in western Montana is characterized by isolated conglomerates, sandstones, siltstones, and dolomitic mudstones and dolostones with development of red-beds in the lower portion, overlain by dolostones and limestones in the upper portions (McMannis 1962; Benson 1966; Meyers 1980). Sparse marine invertebrates indicate an early Frasnian age for the Maywood, with the formation thinning and younging by onlap to the south and east onto the Yellowstone and central Wyoming uplifts (fig. 3; Benson 1966; Hoffman 2020). While the section at Cottonwood Canyon lies south and east of the lap-out of the main body of the Maywood Formation (Sandberg 1961a; Hoffman 2020), it is most parsimoniously associated with the Maywood Formation of western Montana rather than the Souris River of the Williston Basin.

The close relationship between the lower Upper Devonian Maywood Formation and the underlying Lower Devonian Beartooth Butte Formation has been noted by many authors (Sandberg 1961b; McMannis 1962; Sandberg and McMannis 1964; Benson 1966; Zaton et al. 2021). In the southern Montana and northern Wyoming outcrops, these formations sit with significant truncation on

underlying Ordovician and Cambrian units. While these incised units are often interpreted as fluvial to estuarine channel-fills, some exposures appear to represent reworked karst collapse and secondary fill of karst topography on the Lower Paleozoic carbonates (Sandberg 1961b). While the processes filling these features are varied, regionally they represent the in-fill of topography that developed during exposure of the Wyoming platform culminating in a Frasnian highstand and deposition of the Jefferson platform carbonate system (Hoffman 2020).

*Palynology, Paleobotany, and Palynofacies*

Palynological samples were prepared by roughly crushing 5g of samples, placing it within a 500 ml polythene bottle which was then treated with 37% HCl to remove any carbonate and particularly $Ca^{2+}$ that would form an insoluble precipitate when subsequently treated with HF. The sample was then decant washed until neutral and treated with 30 ml of 60% HF acid with the bottle loosely capped to enhance the reaction so as to achieve complete demineralization. The sample was further decant washed and, when neutral, sieved over a 15 µm nylon mesh with the residue being put in a glass beaker. Some 30 ml of 37% HCl was added and the sample was then briefly boiled to solubilize any neoformed fluorides. The sample was then rapidly diluted into 300 ml of water and re-sieved at 15 µm. The organic residue was then stored in a vial and a strew slide made with Elvacite 2044 as the mountant. This revealed that amorphous organic matter (AOM) was dominant in most of the samples which was mostly removed by a 30s treatment with a Sonics and Materials ultrasonic probe. This causes cold boiling by cavitation that preferentially fragments the AOM which can then be removed by a further sieving at 15 µm. To concentrate megaspores, the samples were sieved at 150 µm with the top fraction being again mounted in Elvacite 2044. Two of the samples with the best preserved megaspores were rerun as large sample (60 and 75g) which were disaggregated in 37% HCl. These were then sieved at 150 µm and the sample then further disaggregated by a 45 s treatment with the ultrasonic probe. Part of this residue was also treated for 30 mins in ≥65% $HNO_3$ to clear the sample and remove included pyrite. Two samples were effectively barren of palynomorphs in containing mostly larger plant fragments and rare spores.

Polished blocks were prepared by placing a fragment of rock sample in a mold and then encasing it with the catalytic setting FastGlass resin. Polished thins were made using the method of Hillier and Marshall (1988) by air drying a kerogen suspension in water on a PTFA spray-coated coverslip and then mounting onto a frosted slide. Both blocks and thin sections were successively polished on a 120 diamond lap followed by 3 µm carborundum and then 9.5 µm, 3 µm and 0.05 µm alumina powder

on stationary selvyt laps. Reflectivity measurements and observations were made using a Zeiss UMSP 50 microspectrophotometer using a 40X oil immersion objective [oil with a RI of 1.516) at 546 nm and calibrated with a sapphirine standard (0.413%)]. Fluorescence observations were made on an Olympus BHS-313 equipped with UVFL objectives and a 100W Hg bulb, band pass excitation was 380-490 nm with a dichroic beam splitter at 500 nm and a 515 nm long pass filter.

Mesofossils were extracted by macerating rock samples in 10% HCl until completely dissolved and hand-picking specimens with a pipette under a dissecting microscope. Specimens were dehydrated in an ethanol series and mounted in on slides using Eukitt.

Thin-sections of rock matrix containing charcoal and coprolites were prepared by attaching a cut polished surface of the rock sample to a frosted microscope slide using 2-ton Epoxy; cutting off the excess rock, on a Hillquist thin-section machine, to leave a thin slice attached to the microscope slide; polishing the rock slice down to the desired thickness, on the microscope slide, in the Hillquist machine; finishing the polish with fine grit carborundum; and sealing the slide with a coverslip using Eukitt. Thin-sections, macro- and mesofossils are held in the Humboldt State University Paleobotanical Herbarium (HPH).

## Results

### *The Maywood Formation Measured Section*

An annotated graphic log of the Maywood Formation at the Cottonwood Canyon study site is presented in fig. 4A. This succession has also been described by Sandberg (1963, 1967) and Zaton et al. (2021). Lithologic descriptions are based on field observations as petrographic analysis has not yet been performed. The total measured thickness of the Maywood is 4.85 meters, although the true thickness of the section is uncertain due to cover. The contact of the base of the Maywood with the underlying Upper Ordovician Bighorn Dolomite is not exposed but is constrained to approximately 0.5 meter of covered section. It should be noted that approximately 200 meters east of the measured section across a talus slope is a thick (approximately 33 m) section of conglomerate with red matrix, representing the Beartooth Butte Formation, truncated into the Bighorn Dolomite (Sandberg 1963; Zaton et al. 2021). The Maywood Formation overlaps this Beartooth Butte section and extends further east, as indicated by float of distinctive Maywood lithologies found on the east side of this Beartooth Butte exposure. The Maywood Formation also extends a few hundred meters west of the measured section as these same distinctive lithologies are recognized in float.

The lowest beds ascribed to the Maywood Formation form a small exposure of silty, medium to light gray to tan weathering dolomitic mudstone. It is poorly exposed above a thin covered interval that overlies the Bighorn Dolomite. This unit is divisible into a lower bed exhibiting thin partings overlain by a single, homogeneous bed with slightly sucrosic texture. Highly fragmented plant remains are observed in the upper bed.

A two-meter covered interval overlies this small lower exposure. Above this cover is the main (upper) exposure of the Maywood Formation. The lowest unit in this exposure is a 70 cm dark gray to brownish gray, silty, peloidal dolomitic mudstone. Bedding is poorly developed with indistinct, irregular wavy partings. Subtle but distinct color mottling indicates bioturbation may have homogenized the bedding fabric. Fragmented to larger plant remains are observed in this unit. The overlying 30 cm bed is a dark gray, silty, peloidal, dolomitic mudstone with well-developed planar parallel laminations. Plant material is common to abundant in this bed, accentuating the planar lamination and enhancing fissile partings on weathered outcrop.

The dolomitic mudstone interval is overlain by a 30 cm dark gray, skeletal grainstone. The skeletal fraction is dominated by microconchids, which had previously been described as spirorbid worms from this locality (Sandberg 1963; Zaton et al. 2021). The unit is characterized by planar parallel laminations with some possible development of low-angle, planar stratification. Plant material as charcoal and compressions is abundant in this unit, imparting a fissile parting character to the unit.

A very thin and poorly exposed calcareous mudstone bed separates this lower microconchid skeletal grainstone unit from an overlying 60 cm thick packstone succession. The lower 25 cm is a dark gray-brown to black, peloidal packstone with thin lenses of microconchid skeletal grainstone. Although the peloidal packstone is planar laminated with fissile partings, the thin skeletal grainstones display crude ripple set geometries. Plant material as charcoal and compressions is abundant in this unit.

The overlying 35 cm of this packstone succession is interbedded peloidal packstone and thin microconchid skeletal grainstone. The unit is dark gray to black with planar laminations interwoven with subtle scour-and-fill and ripple set geometries. Plant material is abundant as charcoal and compressions. Fragmentary fish material is also present in this package.

The top of the Maywood Formation is a 35 cm unit of medium gray, silty, peloidal dolowackstone/dolopackstone. Bedding is characterized by very thin, millimeter laminae with subtle scour-and-fill to hummocky stratification. Fragmentary plant material is observed along the laminations. The top of the unit takes on a sucrosic texture near the contact with the overlying Jefferson Formation. Some subtle, low-angle truncation is observed along the formation contact across the outcrop.

233

234 *Palynological Assemblage*

235 The palynological assemblage was investigated by scanning the 16 contiguous palynologically
236 productive samples from the 2 m interval of the upper part of the formation. The spores are generally
237 pale yellow in color and at a very low level of thermal maturity. Vitrinite reflectivity was measured on
238 two samples (#6 and #11). These gave identical results of 0.25% based on 82 and 89 measurements
239 respectively. The samples are rich in AOM so the values will be suppressed but have been corrected
240 (Marshall 1998) to a phytoclast rich equivalent of 0.36%. This is equivalent to a maximum burial
241 temperature of 53°C using the fluid inclusion-calibrated burial heating relationship of Barker and
242 Pawlewicz (1994). The burial depth/temperature has clearly been very low.

243 Preservation is generally excellent although there is some pyrite damage in some of the samples
244 that have a high AOM content. These show a degree of exine homogenisation from preservation in a
245 sapropelic environment. The Maywood Formation is carbonate cemented and the spores have not been
246 as compacted as normally found in clastic sediments. This leaves void space between the spore wall
247 layers that often remains air filled following mounting in Elvacite 2044. This can be advantageous as it
248 reveals the presence of the internal spore wall layer.

249 The palynological assemblage was remarkable in being dominated (fig. 4C) by a single species –
250 *Geminospora lemurata*. Attempts were made to separate this into distinct morphs but, although highly
251 variable in size, based on development of the inner body and the apparent thickness of the outer wall
252 layer in plan-view it conforms with populations described by others (e.g., Playford 1983; Wicander and
253 Playford 1985).

254 As *Geminospora lemurata* was present at over 90% in all the samples (fig. 4C), a standard
255 quantitative count was not attempted since the other components cannot yield statistically significant
256 numbers. Instead, a total slide scan was made to build up a meaningful representation of the other
257 palynomorphs present. The other obvious component is megaspores from *Archaeopteris* (fig. 4B), of
258 which many hundreds are present per g of sample.

259 Other spores include a number with a simple morphology that are present in most samples,
260 including *Retusotriletes distinctus* and *R. pychovii*. There was also a single specimen of a large
261 *Calamospora*. However, as over 14,000 specimens of *Archaeopteris* megaspores were physically counted
262 using a microscope, a few unusual specimens were observed. These included corroded and broken
263 specimens (fig. 5, l & m) that reveal the character of the intexine attached to remnants of the
264 characteristic exoexine. These, if found as isolated specimens, would be clearly identified as

*Retusotriletes distinctus* and *Calamospora*, respectively, but as *Archaeopteris* megaspores they do not add to the diversity.

Both *Insculptspora confossa* (fig. 6 m) and its megaspore-sized equivalent *I. incrustata* (fig. 6, l) are present in a few samples. These are unusual as species in both having a smooth exoexine but a sculptured intexine. A single specimen of *Anapiculatisporites petilus* (fig. 6, j) was also identified.

A persistent component in all the samples is *Cristatisporites cariosus* (fig. 6, k and o) which is probably the most abundant element (between 0 to 3%) after *Geminospora*. This spore type has a very variable morphology and is often degraded, hence the specific epithet. It is identical to the specimens described by Wicander and Playford (1985).

Spores with grapnel-tipped sculpturing are extremely rare, with only two specimens found of *Ancyrospora* (fig. 6, h). These had bifurcate tips (fig. 6, i) rather than being multifurcate. *Hystricosporites* and the other genera sculptured with bifurcate-tipped spines have not been found.

*Aneurospora greggsii* (fig. 6, e) was found in samples 12 and 13. This is not dissimilar to *Geminospora* in size and sculpture, but there is no obvious intexine or inter-layer cavity and it has a thickened equatorial margin that forms prominent curvaturae. *Aneurospora greggsii* is known *in situ* from *Archaeopteris* (Fairon-Demaret et al. 2001) but from the much younger (by ~15 myr) *A. roemeriana* in the upper Famennian of Belgium. *Aneurospora greggsii* is abundant as a dispersed spore in the Upper Famennian of Belgium (Becker et al. 1974) with the clear conclusion (Fairon-Demaret et al. 2001) that it has replaced *Geminospora lemurata* as the microspore of *Archaeopteris*, as the group continually evolved and diversified through the Mid and Late Devonian.

There is one single specimen of *Rhabdosporites langii* (fig. 6, f); this is the *in situ* spore of the aneurophytalean progymnosperms.

A single specimen of *Laiphospora membrana* (fig. 6, g) was found in sample 12. This distinctive monotypic species was reviewed by Playford et al. (1983). It has a late Givetian to late Frasnian stratigraphic range and is only known from Iowa and Canada.

A single specimen of *Cristatisporites triangulatus* was found (sample 16, fig. 6, p) with the distinctive regulate proximal sculpture and inter-radially thinned zona. This is a zonally important form with a stratigraphic range base in the early to mid Givetian to a range top in the late to mid Frasnian (Richardson and McGregor 1986).

Present within many samples and with an abundance in sample 8 are coenobial algae in four-cell primary clusters that are referred to *Musivum gradzinskii* (fig. 6, q). This is a hydrodictyacean chlorococcalean alga known from the Devonian of Poland, Saudi Arabia, China, and North America

(Marshall et al. 2016). Also present in samples 7 and 8 are small numbers of small specimens of the prasinophyte *Lophosphaeridium* (fig. 6, s). There were also two tasmanitid specimens (fig. 6, r), both with thick walls and which, in consequence, remained air filled on mounting in Elvacite 2044. As palaeoenvironment indicators they are generally interpreted as marine but have also been ascribed (Tyson 1995) to a near shore lagoonal environment. A single specimen of *Tornacia* (fig. 6, t) was found that has an age range of early Frasnian to early Viséan (Acritax-JWIP; Playford 1993). No unequivocally marine acanthomorph acritarchs were found in the samples, consistent with the results of R.H. Tschudy, reported by Sandberg (1963).

## Archaeopteris

The microspores of *Archaeopteris*

Genus *Geminospora lemurata* Balme 1962

Type species: *Geminospora lemurata* Balme 1962

*Geminospora lemurata* (Balme) Playford 1983

This species is as described by a number of authors (Playford 1983; Wicander and Playford 1985; Marshall 1996). It also includes the spores described as *Geminospora micromanifesta* var. *minor* by McGregor and Camfield (1982). The spore is relatively small and covered with a sculpture of regularly packed coni. What makes it distinctive is that the exoexine is thin proximally but thickened at least equatorially (fig. 5, d, g, h). This may be an equatorial rim feature or extend further around the body as a distal patina. In addition, the spore contains a smooth inner body (intexine, fig. 5, d, h). This can be obviously developed with a clear separation and hence a cavity (fig. 5, d, g, h) between the intexine and exoexine. Sometimes it can be tightly appressed to the exoexine (fig. 5, a, b, c) so the spore appears as a single wall layered apiculate spore.

Dimensions: Overall equatorial diameter 39 (54) 83 µm, n=107

There has been some confusion with the microspores identified as *in situ* within *Archaeopteris*. This includes the attribution of *Cyclogranisporites* by Pettitt (1965, 1966) that was adopted by Phillips et al. (1972). This is despite an intexine separated from a thickened exoexine being clearly discernible in

some illustrations (Phillips et al. 1972; Plate 45, figs 50, 54). This identification was corrected to *Geminospora* by Allen (1980) but has continued to be requoted (Balme 1995) as an additional and much simpler spore type found within the sporangia of *Archaeopteris*. Further confusion has been added to the *in situ* affinities of *Geminospora lemurata* when a spore with near identical morphology (it differs in that some specimens are tripapillate) was found (Chitaley and McGregor 1988) in a heterosporous lycopod cone. However, it is considerably younger (LN spore zone of the latest Famennian) and with a somewhat different megaspore. It is regarded here as a homeomorph.

Tschudy, in an unpublished report included in Sandberg (1963), noted that the palynoflora from the Maywood Formation at Cottonwood Canyon consisted almost entirely of a single spore *Punctatisporites* cf. *P. planus* of Hacquebard. This is almost certainly *Geminospora lemurata* that had yet to be described at that time.

The megaspores of *Archaeopteris*

1953 *Archaeozonotriletes macromanifestus* Naumova 1953, plate II, fig. 16; plate VII, fig. 1.
1965 Megaspores of *Archaeopteris* cf. *jacksoni* Dawson in Pettitt 1965, Plate 2, figs 1, 6
1970 *Biharisporites maguashensis* Brideaux and Radforth 1970, Plate II, fig. 13
1971 *Contagisporites optivus* (Chibrikova) Owens 1971, Plate XVI, figs 1-6
1972 Megaspores of *Archaeopteris macilenta* in Phillips et al. 1972, plate 45, figs 46-47
1972 Megaspores of *Archaeopteris halliana* in Phillips et al. 1972, plate 43, figs 27, 30, 33, plate 44, figs 34-41, plate 45, figs 43-45.

Spores radial, trilete, camerate. Amb circular to oval to rounded triangular. Exine composed of two layers, the intexine which forms an inner body and the exoexine which completely surrounds it and is attached in the area of the proximal pole. Suturae vary from simple to elevated paired labra. The paired labra are characteristic for the smaller specimens of *Contagisporites* type (fig. 5, I, j, k) less than 250 µm in diameter. On these smaller specimens the labra are joined to, and connected by, a prominent curvatural ring. The line of this curvatural ring is apparently coincident with the boundary of the intexine and exoexine attachment. On larger specimens there are less prominent labra (fig. 5, p, q) that terminate in curvaturae imperfectae. The largest specimens (fig. 5, t, u) have simple suturae and no curvaturae. The presence of curvaturae and elevated suturae labra is not mutually exclusive with maximum size. There are smaller spores with thin labra and curvaturae (fig. 5, figs q, r) and small spores

that have simple suturae and inconspicuous curvaturae (fig. 5, fig. n). The intexine is thin walled and usually quite conspicuous. The exoexine is obviously thicker walled – some 4 (9) 19 µm thick (n=40), measured on the equatorial section. The exoexine outside the contact area is sculptured with close packed coni and grana. These are conical to biform and include forms ascribed to the varieties *C. optivus optivus* (fig. 5, o, s, t, u) and *C. optivus vorobjevensis* (fig. 5, r). The larger specimens are more frequent broken and fragmentary.

Dimensions: are given as min (mean) max of maximum equatorial diameters of exoexine and intexine. Dimensions are for spores with curvatural rings placed in *Contagisporites optivus*, and then the larger forms without distinctive curvaturae. Results are also given for the combined population. These measurements are in approximate proportion to their relative abundance. The exoexine and intexine diameters are cross-plotted on fig. 7 with exoexine sizes also presented as a histogram.

| | |
|---|---|
| All megaspores | 220(349)548; 124(271)472 µm n= 201 |
| *Contagisporites* | 220(280)376; 124(181)268 µm n=76 |
| larger spores | 208(327)472; 252(391)548 µm n=124 |

*Discussion*. Observation of a large number of the megaspores shows a continuous variation from smaller specimens that are clearly *Contagisporites* to larger specimens that have usually been referred to *Biharisporites*. This linkage has been recognised before both in the bulk macerated population of Phillips et al (1972) and by Allen (1980) based on a dispersed population from the Givetian of Ella Ø, East Greenland that he regarded as originating from the same or related parent plants. The maximum equatorial diameter distribution (fig. 7) shows a continuous distribution between spores that have elevated labra and curvatural rings that would be identified as *Contagisporites* if found as dispersed spores and the larger megaspores that have weakly developed or lack curvaturae.

There has been considerable and continuing confusion as to the identity of the megaspores of *Archaeopteris*. This is often the result of early identification when the descriptive terminology of dispersed spores was in its infancy, and has been advanced as an argument that the palynological based taxonomy does not map onto the palaeobotanical one, with many different genera present within single sporangia. It is useful at this point to review the taxonomic history of the megaspores.

The first megaspores were described from *Archaeopteris* by Arnold (1939), from the lower Pocono of Pennsylvania. Subsequently, Pettitt (1965) described megaspores from other specimens of *Archaeopteris* reported by Arnold (1936) from the early Frasnian (McGregor 1996) of Escuminac,

Quebec and the Late Devonian at Port Allegany in Pennsylvania (Arnold 1939). Pettitt (1965) placed these megaspores within *Biharisporites*. This was a genus erected by Potonié (1956) to replace the monogeneric spore genus *Triletes* (as *T. spinosus*). *Biharisporites* was defined as a megaspore sculptured with densely packed coni, having an internal body and a curvatural feature that can be distinct. The type species is from the Early Permian of Gondwana and has been subsequently emended three times, most recently by Glasspool (2003). In the 1960's *Biharisporites* was used several times for what are now regarded as distinctly different megaspores including *B. ellesmerensis* (now *Verrucosisporites ellesmerensis* and the co-occurring megaspore of the arborescent lycopod *Protolepidodendropsis;* Berry and Marshall 2015) and *B. parviornatus* (Richardson 1965) from the Eifelian of Scotland. *Biharisporites parviornatus* is not relevant here as it predates the inception of the archaeopteridalean progymnosperms. Despite this, *B. parviornatus* was used as a name for the *in situ* spores of *Archaeopteris* (Phillips et al. 1972). *Biharisporites* was also used by Vigran (1964) for a new megaspore species from the Givetian of Spitsbergen (*B. spitsbergensis*) that had been earlier identified by Høeg (1942) as Granulati type a. Vigran included within the species spores with a very distinctive curvatural ring accompanied by paired labra that are thickened at the intexine-exoexine contact, as well as larger specimens with the same sculpture and intexine but with much less distinctive curvaturae. Allen (1965) studied spore assemblages from the same section and recognised that the same spore had been previously described by Chibrikova (1959) as *Archaeozonotriletes optivus*, with a new variety (*A. optivus vorobjevensis* with coarser and denser sculpture) being subsequently added (Chibrikova 1962). Allen (1965) accepted *A. optivus* as the senior synonym but placed it with the genus *Calyptosporites*. The same species was also described by Taugourdeau-Lantz initially (1960) as *Retusotriletes* sp and then in 1967 as *Rhabdosporites cuvillieri*.

In 1971 Owens used the combination of the distinctive curvaturae coupled with a thick exoexine to create the new genus *Contagisporites* with the varieties *optivus optivus* and *optivus vorobjevensis*. *Contagisporites* was illustrated for the first time from *Archaeopteris* by Phillips et al. (1972) – as the megaspore of *Archaeopteris* (plate 43 fig. 24 and plate 44, fig. 38 of Phillips et al. 1972) – in their study of two heterosporous species of *Archaeopteris* from the Upper Devonian of West Virginia. As they had only limited success with spore recovery from sporangia, the description was mostly based on bulk maceration of the matrix that enclosed *Archaeopteris* fronds. These megaspores were not given names from the dispersed spore literature but placed in open nomenclature. The attribution of the West Virginia megaspores to *Contagisporites* was made subsequently in a review of Late Silurian and Devonian *in situ* spores by Allen (1980).

*Contagisporites* has now been widely recognised in Givetian palynological assemblages from across Euramerica. It has been used to define the latest Givetian OK palynological zone (Avkhimovitch et al. 1993; Turnau and Racki 1999) although it does appear somewhat earlier (Marshall 1996). However, the larger *Biharisporites* is rarely recorded although it is probably the spore figured as the new species *Biharisporites maguashensis* by Brideaux and Radforth (1970) from the Escuminac Formation of Quebec and particularly the specimen subsequently illustrated by Cloutier et al. (1996, Plate II, fig. 2). However, it should be noted that the bulk of the specimens measured from the Maywood Formation do not possess a strong curvatural features and so cannot be placed within *Contagisporites*.

One spore that has not been discussed with respect to *Archaeopteris* is the megaspore *Archaeozonotriletes macromanifestus* described by Naumova (1953) from the Givetian and early Frasnian of Russia. Naumova (1953) reports its size as between 100-200 µm in diameter although its scaling relative to other spores on the plates suggests it is much larger. It has been reported and figured largely from Russia (e.g. *A. macromanifestus* var. *angulatus* of Chibrikova 1962), where it can be compared with the line drawing of *Contagisporites optivus* that is on the same plate (Chibrikova 1962 plate XI, figs 5-6). *Archaeozonotriletes macromanifestus* has similar sculpture but differs in being somewhat larger and lacks the elevated labra or distinctive curvatural ring. It has also been figured by Braman and Hills (1992) from the Upper Devonian of the Northwest Territories, Canada. *Archaeozonotriletes macromanifestus* both conforms to the description of the larger megaspores from *Archaeopteris* and has the same morphological relationship to *Contagisporites*. It is interpreted here as a hitherto unrecognised dispersed megaspore of *Archaeopteris*.

Dispersed spore taxonomy has generally been an artificial system based solely on morphology and to the exclusion of information from sporangia that shows what the natural range of variation within a particular sporangium should be. This range of variation does not map onto spores as described from dispersed populations. Conodont workers faced this dilemma (Knell 2012) in moving from a taxonomy based on isolated elements to one based on the complete conodont jaw apparatus. Clearly the issues faced in dispersed spore taxonomy are of a much greater magnitude in that the *in situ* information or even dispersed sporangia that contain bundles of natural taxonomic information is missing for most spores, although generally not for the major plant groups within floras. If we were to adopt such a system, the megaspores of *Archaeopteris* would, by priority and using form genera, become known as *Archaeozonotriletes macromanifestus*. This conforms with the intent of Russian palynologists who largely put the camerate spores with minor sculpture and thickened distal exoexines (i.e., the spores of progymnosperms) into *Archaeozonotriletes*. It was unfortunate that Potonié (1958)

chose the first illustrated specimen to become the type species *Archaeozonotriletes variabili*s, an atypical form that is not of progymnosperm affinity. This potential emendation of *A. macromanifestus* would also include *Contagisporites* as immature less developed specimens.

As regards broadening the definition of *Contagisporites* to include forms without the prominent labra and curvatural ridge, this would significantly change the definition of a genus that is widely recognized, distinctive and an important zonal marker. So, it would be better to make such an emendation as part of a general taxonomic revision of both progymnosperm macrofossils and their *in situ* and dispersed spores.

Although *Biharisporites* is a morphologically based genus that can be used throughout the geological column, its re-emendation (Glasspool 2003) has very much aligned it with a group of unrelated Permian megaspores from Gondwana that significantly post-date the extinction of the progymnosperm group. So, it is inadvisable and has been the cause of significant confusion to misapply this name to a group of somewhat different unrelated Devonian megaspores.

It is of note that *Contagisporites* has been reported frequently in the Devonian spore literature in contrast to the larger-sized *Archaeopteris* megaspores. In part, this may be because the larger size of the latter renders them more prone to breakage and, consequently, less likely to be recovered regularly in routine palynological residues. If found, these larger megaspores would be simply noted as a not very distinctive type of megaspore. In contrast, *Contagisporites* is distinctive and with its prominent curvatural ring is robust. It is also normally the largest spore when found in routine palynological processed preparations. So, it is likely that the larger *Archaeopteris* megaspores were too large to become widely dispersed, so it is only when samples are taken in close proximity to the source plants that this type is recovered in noticeable quantity.

### *Macroflora*

The plant meso- and macrofossils consist of fragments of charcoalifed wood (fig. 8, 10E-10G, supplemental fig. 1A), adpressions of axes (fig. 8F, 9, 10A, 10B, supplemental fig. 1B, 2E), foliage (fig. 10C, 10D, supplemental fig. 2A), and sporangia (or sporangium contents) (fig. 11E-11H). Mesofossils hand-picked following acid-dissolution of rock samples include dehisced sporangia (fig. 11A, 11B, supplemental fig. 2B), clumps of spores released from sporangia (fig. 11C, 11D, supplemental fig. 2C, 2D), and seed-megaspores (fig. 12A-12E). At macroscopic scales, the plant material is highly fragmented and specimens large enough to present diagnostic characters are rare. One exception is a horizon that

preserves a dense mat of compressed intertwined leafy axes (fig. 9D-9F), but there the oxidation of the material has obliterated many diagnostic characters.

The charcoalified wood occurs as fragments of varied size – from a few millimeters to several centimeters across (fig. 8, 10E-10H, supplemental fig. 1A). Many of the large charcoal fragments are rounded, oblate, and deposited with their two long axes parallel to the bedding planes (fig. 8B, 8D, 8E, supplemental fig. 1A). Examination in scanning electron microscopy and petrographic thin sections reveals tracheids with grouped pitting (fig. 10H) consisting of circular bordered pits with oblique slit-shaped apertures, and uniseriate rays of low height (fig. 10F, 10 G). These are all typical of *Callixylon*-type wood of archaeopteridalean progymnosperms, reported from Cottonwood Canyon by Sandberg (1963).

Charcoal also occurs as charred axes of diverse sizes, from a few millimeters to several centimeters across (fig. 8A, 8E, 8F). The axes are compressed fragments, often with rounded ends (fig. 8E). They occur with high frequency in a few horizons of the sedimentary sequence, usually in association with the larger charcoalified wood fragments (fig. 8E). The charcoal of the axes is crumbly and tends to disaggregate, which leaves behind impressions of axes harboring small bits of charcoal and orthogonal lattices of fine veins formed by diagenetic mineral precipitation (fig.8E, 8F).

Most of the axes preserved as carbonaceous compressions are non-descript relatively short fragments (up to c. 10 cm) that do not exhibit appendages or branching (fig. 8C, 8F, 9A-9C). They are c. 1-20 mm wide, some with rounded ends, and may be more or less oxidized, depending on the sedimentary facies of the host layer (fig. 9). Two specimens warrant special note. One is an axis fragment 6.5 cm long and 3 mm wide, branched dichotomously and bearing a few irregularly-spaced bases of lateral appendages c. 0.5 mm wide (fig. 10A). The habit of this axis is reminiscent of plants of the cladoxylopsid plexus, but the specimen does not exhibit sufficient diagnostic characters. The second specimen is a 6.5 cm long fragment of a very thin axis (up to 1 mm wide) with undulating habit and isotomous branching (fig. 10B) that falls under the broad taxonomic umbrella of the form-genus *Hostimella*.

Aside from the charcoalified wood, the most taxonomically-relevant information comes from sporangia and clusters of spores, and from a dense mat of compressed leafy axes (fig. 9D-9F). Because the axes are densely intertwined in large numbers and relatively heavily oxidized (fig. 9D), and probably also because of the morphology of the leaves themselves, entire leaves are very difficult to individuate, despite the size of the rock sample examined. The leaves are fan-shaped, long and narrow, and dissected into long strap-shaped lobes (fig. 10C, 10D, supplemental fig. 2A). Insofar as it can be

ascertained, they have open dichotomous venation, with veins branching at very high angles, which renders basal portions of the leaves and the strap-shaped terminal leaf lobes very similar to the axes that bear longitudinal striations. Additionally, the preservation of the axes is sub-optimal and some are split longitudinally at some places (fig. 9E), which are similar to the points of leaf dissection. The leaves are c. 1.6 cm long (some may be longer), 1 mm wide at the base, with a distal portion up to 5 mm wide, and with the tips of the distal lobes rounded (fig. 10C, 10D). Because of the reasons listed above, the attachment of leaf bases to axes is also hard to demonstrate unequivocally (fig. 9F).

The sporangia are fusiform and small, 1.0-1.8 mm long and 0.4-0.7 mm wide, with an epidermis consisting of long, narrow cells aligned parallel with the long axis of the sporangium (fig. 11A, 11B, supplemental fig. 2B). Most of the sporangia recovered by rock maceration are dehisced along a line that runs the entire length of the sporangium (fig. 11A). Together, these features are consistent with those of progymnosperm sporangia. On bedding planes, sporangia are found isolated (fig. 11E-11G), with a few exceptions. In one case, a sporangium is attached to an axial fragment, probably part of a sporophyll (fig. 11G). In another case, four sporangia of the same type, all fragmentary, occur parallel to each other, forming a file (fig. 11H), similar to the positioning of sporangia typical of progymnosperm sporophylls. Consistent with all these progymnosperm similarities, the material recovered by rock maceration includes fusiform clusters of archaeopterid microspores and megaspores that represent the undissociated contents of sporangia (fig. 11C, 11D, supplemental fig. 2C, 2D). Similar clusters of microspores are also seen on bedding planes, sometimes in dense aggregations (fig. 11I), whereas the megaspores (300-360 µm in diameter) are often found isolated on bedding planes (fig. 11J, supplemental fig. 2E), sometimes in abundance (supplemental fig. 2E).

Aside from the typical archaeopterid reproductive structures, we have observed a large isolated spinose spore (c. 1.4 mm diameter; fig. 11K) reminiscent of *Ancyrospora* (although it does not display sufficient diagnostic characters) on a bedding plane, and seed-megaspores (fig. 12). Like those originally described by Marshall and Hemsley (2003) as *Spermasporites allenii*, the seed-megaspore complexes recovered by rock maceration consist of a large functional megaspore, three abortive megaspores, and agglomerations of microspores covering the abortive megaspores (fig. 12A, 12G). The functional megaspores, 670-930 µm in polar diameter and 480-650 µm in equatorial diameter, exhibit a trilete mark at the proximal pole (fig. 12F, 12H) that is open in one of them (fig. 12H), which also contains a conspicuous dark inner body (fig. 12B). The microspores are 40-50 µm in polar diameter. Two of the seed-megaspore complexes are covered partially or entirely by an outer wall layer (fig. 12A, 12D), which shows characteristic longitudinal folds (fig. 12A). An isolated teardrop-shaped structure observed on a

552 bedding plane (fig. 12E) is probably a seed-megaspore or its separated external wall layer, as this
553 structure has shape and size comparable to those of the seed-megaspore complexes from rock
554 macerates, including marks similar to the longitudinal folds in their outer wall layers.
555
556 *Fauna*
557 The fauna includes microconchids (described by Zaton et al. 2021; see also the discussion
558 section below) and fishes. Sandberg (1963) reported from the Maywood at Cottonwood Canyon fish
559 remains identified by F.C. Whitmore and D.H. Dunkle as *Bothriolepis*, heterostracan and coccosteid
560 plates, palaeoniscoid teeth, and *Holoptychius*. We observed fragmentary fish dermal skeletal elements
561 including plates and scales, as well as coprolites possibly produced by fishes.
562 A scale fragment sectioned vertically in a thin section (fig. 10E, 13A) resembles, at least
563 superficially, the described cosmoid scale histology of sarcopterygians, such as *Holoptychius* (Mondéjar-
564 Fernández and Meunier 2021), a genus previously documented in the Maywood Formation. Cosmoid
565 scales are characteristic of sarcopterygians (Mondéjar-Fernández and Clément 2012; Mondéjar-
566 Fernández and Janvier 2021), and have a network of vascular and pulp cavities and canals between an
567 inner bony layer with narrow vascular canals and an external cosmine layer (Schultze 2016). Our
568 specimen (fig. 13A), 1.2 mm thick, shows the network of canals underlain by a thick dense bony layer,
569 but because of incomplete preservation it is unclear whether the cosmine layer is present. *Holoptychius*
570 has a reduced to absent cosmine layer (Mondéjar-Fernández and Meunier 2021), so it is possible that
571 this fragment actually represents this genus.
572 A second scale, uncovered on a bedding plane (fig. 13B, supplemental fig. 3A), is also from a
573 sarcopterygian, based on the round outline (Mid and Late Devonian actinopterygians generally have
574 rhomboid scales). The scale is 9 mm across, with fine anteroposteriorly oriented ridges on the posterior
575 edge, low tubercles in the anterior area, and covered by a thin shiny enamel layer. Among the
576 sarcopterygians recognized in the Maywood Formation, the porolepiform *Holoptychius* has rounded
577 scales that appear to lack cosmine, and the dorsal and flank scales of the genus have anteroposteriorly
578 oriented bony ridges (Mondéjar-Fernández and Meunier 2020). However, this scale is not as heavily
579 ornamented and not nearly as thick as the scales of *Holoptychius*. This scale is more similar to those of
580 tetrapodomorph fishes, such as rhizodonts and tristichopterids (Mondéjar-Fernández, pers. comm.,
581 December 2021). These groups were present throughout the Mid and Late Devonian but their members
582 are very difficult to distinguish exclusively based on isolated scales.

583 Elongated, dark brown objects interpreted as coprolites occur on bedding planes. One of them is
584 large (9-10 mm in diameter and more than 7 cm long) and crossed by an orthogonal network of fine
585 diagenetic mineral precipitation veins (fig. 13C, 13D, supplemental fig. 3C). It consists of amorphous
586 material that forms a "swirly" texture around "nests" of angular fragments up to 700 µm in size (fig. 13E,
587 13F, supplemental fig. 3B). Careful scrutiny in thin sections demonstrates absence of any plant material,
588 which indicates that this coprolite was not produced by an herbivore.
589
590 **Discussion**
591 *Age of the Maywood Formation*
592 *Palynostratigraphy*. Zaton et al. (2021) interpreted the age of the Maywood Formation as mid
593 Givetian based upon the presence of *Geminospora lemurata* and rare specimens of *Cristatisporites*
594 *triangulatus* (as *Samarisporites*). In the context of this somewhat older age estimate than suggested by
595 the conodont calibrated sequence stratigraphy (Zaton et al. 2021), it is useful to discuss age evidence
596 from our palynological assemblage. Given the extremely low diversity of the assemblage, it is important
597 to understand the regional comparisons with previously described assemblages (Fig. 14), in addition to
598 using global schemes that are typically based on diverse assemblages. Usefully, these regional
599 palynology records form a mid Givetian to late Frasnian series of assemblages. The situation in the
600 American Midwest is quite testing for palynology in that the sequence is dominated by platform
601 carbonates to the detriment of fine-grained clastic sediment and, in consequence, to palynological
602 preservation.
603 Spores have been described (Peppers and Damberger 1969) from the thin Wapsipinicon Coal (~1
604 cm) in the Davenport Limestone Member of the Wapsipinicon Limestone Group of central Illinois. This is
605 now placed within the *ansatus* conodont zone and Iowa Basin T-R cycle 2c (Day and Witzke 2017; Day et
606 al. 2006). The Wapsipinicon Coal contains a diverse assemblage including bifurcate-tipped spores,
607 diverse *Grandispora* and *Rhabdosporites langii*. The most common elements are new species of
608 *Apiculatasporites*, *A. wapsipiniconensis* and *A. davenportensis*. Careful scrutiny of the illustrations in
609 Peppers and Damberger (1969) indicates that these specimens are almost certainly *Geminospora*
610 *lemurata* in which the characteristic inner body was not recognized. The coal is vitrinite rich (Peppers
611 and Damberger 1969) so, given the abundance of *Geminospora*, the Wapsipinicon Coal will represent
612 the development of autochthonous *Archaeopteris* vegetation on a carbonate platform. There are rare
613 acanthomorph acritarchs (*Veryhachium octoaster*) that indicate a very minor marine influence.

Another spore assemblage has been described by Sanders (1968) from the Cedar Valley Coal, which is similarly thin (~2-5 cm), and from within the lower part of the Coralville Formation of Iowa City, Iowa. This is now attributed to the upper *disparilis* conodont zone of late Givetian age and to Iowa Basin T-R cycle 4 (Day and Witzke 2017). The assemblage is diverse and contains abundant *Geminospora lemurata* with *Ancyrospora*, *Rhabdosporites langii* and *Laiphospora membrana*. Dow (1960) describes the coal as a cannel coal, with what is recorded as a hydrocarbon element in thin sections that is presumably AOM. In this respect it is comparable to our AOM-rich samples from Cottonwood Canyon and again represents an *Archaeopteris* flora on a carbonate platform.

A further assemblage was reported by Guennel (1963) from a fissure filling in the Mid Silurian Tilden Reef, in western Illinois. In common with the other two short accounts, it contains a number of new species that are probably junior synonyms. The assemblage includes *Geminospora lemurata* (as *Stenozonotriletes bellus*, with the genus reported as abundant), *Rhabdosporites langii* (as *R. firmus*), *Ancyrospora* (as *A. simplex*, probably *A. incisa*) and *Cristatisporites intermedius* (possibly *C. cariosus* of Wicander and Playford (1985), in which case it would be the senior synonym). The age of this assemblage is less certain but it was reappraised by McGregor (1979) and seen as similar to a conodont-dated spore assemblage from the Long Rapids Formation of northern Ontario, of early to mid Frasnian age. The abundance of *Geminospora* again indicates an *Archaeopteris* flora growing on a basement of Silurian limestone.

McGregor and Owens (1966) figured spores from the Escarpment Formation of Northwest Territories, Canada that was dated with brachiopods as mid-Frasnian *albertensis* zone age. The assemblage includes *Geminospora lemurata*, *Laiphospora membrana*, *Ancyrospora* spp and *Archaeoperisaccus* spp. *Archaeopteris* megaspores are present as ?*Archaeozonotriletes macromanifestus* with the characteristic thickened labra of *Contagisporites optivus*. This assemblage is much further north (Fig. 14) and into the palaeolatitudes where *Archaeoperisaccus* was present.

The only account of spores from a longer stratigraphic section is that of Wicander and Playford (1985), from a series of exposures of the Lime Creek Formation of northern Iowa. This is placed by Day and Witzke (2017) in the late Frasnian and as Iowa Basin T-R cycle 7A. It is from the lower *Palmatolepis gigas* conodont zone and also contains the ammonite *Manticoceras regulare*. The palynological assemblage is very much dominated by acritarchs. The lower diversity spore flora includes abundant *Geminospora lemurata* together with *Cristatisporites cariosus* and *Laiphospora membrana*. *Ancyrospora*, *Grandispora* and other characteristic late Frasnian spores are absent.

The significant question in interpreting the age of the Maywood Formation palynological assemblage is whether it represents either an ecologically very restricted assemblage from a flora that can tolerate growing on a carbonate platform in an arid climate, or it represents the typical contemporary Euramerican spore assemblage. The abundance of *Geminospora* may also be compounded by *Archaeopteris* likely being a spore super-producer, as a long-lived plant with abundant, small sporophylls that were probably abscised periodically. In contrast, cladoxlyopsids such as *Wattieza* (e.g., Stein et al. 2007), which represent another important component of Devonian vegetation at the global scale, had a different growth habit that probably led to comparatively smaller spore output. The Wapsipinicon, Cedar Valley and Tilden Reef palynological assemblages are from a near-identical palaeoenvironmental situation of *Archaeopteris* growing on a carbonate substrate within the same arid climate zone. They show an absolute abundance of *Geminospora* but more significant palynological diversity, with the other main groups of Devonian plants represented in the palynoflora. Thus, the absence of this spore diversity from the Maywood Formation palynological assemblage implies that it is younger in age. Wicander and Playford (1985) interpreted the Lime Creek Formation terrestrial palynomorph assemblages as very impoverished in terms of diversity and attributable to a nearshore open marine palaeoenvironment. Their conclusion of an open marine environment is entirely in accord with the presence of ammonoids and conodonts at the sampled localities. However, the assemblage is not too different from that of the Maywood Formation in terms of the abundance of *Geminospora*, persistent presence of *Cristatisporites cariosus*, presence of *Laiphospora membrana* and an absence of *Ancyrospora* and *Grandispora*.

Of the age diagnostic species present in the Maywood, *Cristatisporites cariousus* is only known from the Frasnian (plus a non-figured, out of range, latest Famennian record in a metamorphosed palynological assemblage from Cornwall in the UK; Sellwood et al. 1993), and *Laiphospora membrana* from the late Givetian to late Frasnian (Playford et al. 1983). This implies that the early Frasnian age determined from sequence stratigraphic analysis of the conodont-dated overlying Jefferson Limestone is broadly correct. This early Frasnian age can also be interpreted in the context of the late Givetian Taghanic Event that caused significant extinctions (Abousallam and Becker 2011) in both the terrestrial and marine environments. In late Givetian arid zone palaeolatitudes on the Old Red Sandstone Continent, the sustained aridity (Marshall et al. 2011) associated with the extinction led to the disappearance of most spore diversity, resulting in a flora that was dominated by *Geminospora*, i.e. *Archaeopteris*. Bracketing this episode of aridity are two very significant marine transgressions with the upper being the Taghanic Onlap. This would have drowned out much of the remaining flora on the

carbonate shelves of the American Midwest. The combined effect would have been a depleted flora of *Archaeopteris* as the significant surviving element that was then able to spread across the carbonate shelf during times of relative low stand.

*Regional paleogeography and stratal relationships*. Regional stratigraphic relationships also argue against a Givetian age for the Maywood Formation in Cottonwood Canyon. The Souris River Formation may be as old as Givetian in the central part of the Williston Basin of North Dakota and northward into Canada (Sandberg 1961a) but is progressively younger by onlap out of the basin and onto the south and central arch region of central Montana and Wyoming. Likewise, Middle Devonian strata to the west are limited to Idaho and Utah with potential Givetian-aged strata in western Montana limited to displaced sections carried eastward on Overthrust Belt allochthons (Johnson et al. 1988, Grader and Dehler 1999). Like the Souris River, the Maywood thins by onlap to the south and east, thus becoming younger toward the Wyoming platform region. Thus, if the Maywood Formation in Cottonwood Canyon was in fact Givetian in age, it would be detached from any coeval marine Middle Devonian successions to the northeast and northwest by upwards of 200 kilometers, and would represent an older, isolated, fully continental setting, in which case it would not be genetically related in any way to the lower Frasnian Maywood succession of southern Montana. The Frasnian age estimate for this deposit makes it truly coeval with, and genetically related to, the Montana Maywood succession. These freshwater-dominated to nearshore marine deposits of the Wyoming and southern Montana Maywood Formation are the initial onlapping succession associated with the long term Frasnian transgression that would flood the southern Montana and northern Wyoming arches, culminating in deposition of the Jefferson carbonate platform.

## *The Maywood Formation Flora and Vegetation*

The meso- and macrofossils of the Maywood plant assemblage that exhibit taxonomically diagnostic characters (sporangia and charcoalified wood) point to archaeopterid affinities of most elements of this flora. This inference receives strong support from the palynoflora, overwhelmingly dominated by *Archaeopteris* spores. This implies that the foliar material is also likely archaeopteridalean. Indeed, all *Archaeopteris* species possess cuneate leaf bases, if not leaves that are fan-shaped altogether, like those present in the Maywood. However, Devonian fan- or wedge-shaped leaves (also referred to as cuneiform of flabelliform) fall under a number of genera, including (but are not limited to) *Eddya*, *Platyphyllum*, *Psygmophyllum*, *Ginkgophyton*, *Enigmophyton*, *Germanophyton*,

*Thamnocladites*, and *Flabellofolium*. Some of these have demonstrated or putative affinities with the archaeopterids, while others are morphology-based organ genera (some of which are nomenclatural labyrinths; e.g., Høeg 1942; Beck 1963, 1970; Stone 1973). As a result, the lines separating these genera are often blurry. Because of these taxonomic uncertainties, and due to the lack of sufficient diagnostic characters, we cannot propose an unequivocal taxonomic placement for our foliar material. Nevertheless, we note that circumstantial evidence points strongly to archaeopteridalean progymnosperms, and that this material is most similar to *Archaeopteris notosaria* (Anderson et al. 1995) and *A. sphenophyllifolia* (Arnold 1936; Kräusel and Weyland 1941; Orlova et al. 2016), but also to *Thamnocladites vanopdenboschii* (Stockmans 1968), all of which are known from the Upper Devonian.

The overwhelming dominance of the archaeopterids in the fossil assemblage leaves little room for doubt about a vegetation consisting largely of monospecific forest stands. The abundance of archaeopterid charcoal indicates high incidence of wildfires. The presence of a *Hostimella*-type axis (fig. 10B) and presence among the palynomorphs of *Spermasporites* seed-megaspores (fig. 12) alongside rare non-archaeopterid spores of other types, indicates that a few other plant types were present in small numbers in the area. Additionally, the Wyoming occurrence of *Spermasporites* extends the geographic range of the (unidentified) plant group that produced seed-megaspores. This range currently encompasses all of Euramerica, from Wyoming to Russia and north to Greenland (Marshall and Hemsley 2003), and demonstrates that these plants were widely distributed and could thrive on the arid carbonate platforms of western Laurentia. Despite the abundance of archaeopterid remains, including relatively large charcoal fragments, large trunks typical of *Archaeopteris* are absent. This could be due to the limited exposure at Cottonwood Canyon or to the decomposition of trunks in situ, in the arid climate of the area, but it is also possible that the Maywood archaeopterids had smaller stature and a shrub-like habit, growing mangrove-like in along the margins of the Maywood basin (lagoon).

An obvious question regarding the low-diversity vegetation represented by the Maywood flora, is whether it reflects tight ecophysiological constraints driven by the environment – plants that can grow on an arid carbonate platform – and geographic position – far west of the centers of diversity at the time (e.g., eastern Laurentia; Stein et al. 2012) –, or is it telling us about age? Comparable palynomorphs assemblages from Illinois and Iowa (Guennel 1963; Sanders 1968; Peppers and Damberger 1969) (fig. 14) are more diverse despite being from within platform carbonates. However, these assemblages are slightly older, Givetian (McGregor 1979; Day and Witzke 2017). On the other hand, the Lime Creek Formation flora (Wicander and Playford 1985), an early Frasnian palynomorph assemblage from the same region (Iowa) representing carbonate platform vegetation in the vicinity of a marine basin, is

741 impoverished, like the Maywood palynoflora. Based on these, we suggest that the Maywood
742 assemblages represent archaeopterid forests with little understory vegetation, spread across the
743 carbonate platform in the vicinity of the Maywood basin.
744
745 *Depositional Environments of the Maywood Formation*
746 *Evidence from the sedimentary facies*. The very limited exposure of the Maywood Formation in
747 Cottonwood Canyon makes interpreting the original dimensions of the deposit difficult, if not
748 impossible. However, the close association of the Maywood with the underlying Beartooth Butte
749 Formation indicates the Maywood occupied local low topography originally created by some
750 combination of karst and fluvial erosional processes preceding and during Beartooth Butte deposition
751 (Sandberg 1961b). This local incised channel-form would have been surrounded by plains of Bighorn
752 Dolomite, in essence a regional pediment dipping to the northern Souris River/Maywood marine basins.
753 Potential beveling of the Bighorn Dolomite by the Frasnian transgression that subsequently deposited
754 the Jefferson Formation may have subdued the relief originally present during deposition of the
755 Maywood, but as presently observed this relief is subtle.
756 Whether this thin deposit represents the margin of a thicker Maywood channelized system that
757 has been removed by recent erosion of Cottonwood Creek, or it records the entirety of a thin Maywood
758 depositional system, is open to speculation. That said, this exposure of the Maywood Formation
759 contains no extra-basinal terrigenous sediment (i.e. siliciclastic sand or bedded silt) packaged within
760 traction or suspension beds that might indicate deposition in a fluvial margin splay/levee setting (Bridge
761 2006). Likewise, no surfaces internal to the Maywood Formation are recognized exhibiting rooting or
762 alteration that might suggest an exposed overbank/floodplain setting. Given this lack of suggestive
763 sedimentary evidence, it does not appear the Maywood deposit was associated with channelized fluvial
764 or estuarine deposition.
765 The carbonate mud-dominated lithologies of the lower Maywood Formation at the study site
766 suggest deposition in a low energy setting. While mottling in some of these carbonate mudstones
767 indicates sediment re-working by burrowing organisms, the abundance of organic matter and the
768 presence of pyrite demonstrates some level of oxygen depletion in the system, with at least reducing
769 pore-waters in the early, shallow burial realm (Berner 1985). The planar laminated mudstone beds may
770 have been deposited on sub-aerial mud flats, however there is no evidence of desiccation cracks,
771 breccias, or other indicators of exposure in these facies. Thus, deposition of the lower Maywood

Formation appears to have been in a low energy, fully sub-aqueous environment that experienced some level of bottom water restriction and oxygen depletion.

The skeletal and peloidal, grain-dominated carbonate lithofacies that overlie the mud-dominated facies represent a relative shallowing of the depositional system to local wave-base or current-swept conditions. The planar parallel-laminated beds are typically associated with wave-dominated, foreshore environments (Inden and Moore 1983), representing either the swash zone of a bar or an attached, fringing beach system. The ripple, hummocky, and low-angle scour and fill stratification styles represent traction transport and deposition of grains in an environment experiencing a mixture of current-and wave-dominated processes (Inden and Moore 1983). These bedforms are typical of the upper shoreface immediately offshore of the foreshore/beach. The interbedding of planar parallel and cross-stratified grain-dominated lithologies strongly suggests the upper portion of the Maywood Formation was deposited in the upper reaches of a wave-dominated environment, potentially as a beach system developed along the edge of the incised channel complex.

While the presence of grain-dominated, planar and cross-laminated carbonates indicates deposition in a wave-dominated setting, the thickness and scale of these beds and bedforms are quite small (1 – 20 cm maximum), suggesting this deposit represents a local system with minimal fetch, thus a relatively quiet, low-energy shoreface. Even if the original deposit extended across modern Cottonwood Canyon and was eroded, the deposit would have been less than a kilometer in width. The length of the channel complex itself is also unresolved but would have to extend over 100 kilometers to the northwest to meet confirmed shallow marine Maywood Formation in southwest Montana (Meyers 1980).

*Evidence from the palynofacies*. The palynofacies is dominated by AOM, with spores being the next most conspicuous element. Also present as a minority component are phytoclasts that are generally small and equant. Observation of polished thin sections in reflected light preparation shows these phytoclasts to be vitrinite, i.e., plant material that has collapsed to a gel in the AOM rich environment. Much rarer is charcoal that is identified as inertinite or semi-fusinite. Size sieving of the palynological samples at 150 µm revealed no intact sporangia, sporangial fragments and only clusters of microspores. There were a few samples that contained very few palynomorphs. These are from the layers with richest in recognizable archaeopterid remains and had significantly more phytoclasts and particularly larger fragments of charcoal. Also of importance is that the palynological assemblage and

palynofacies in all the samples through the upper meter of the Maywood Formation is essentially similar. So, the environment was stable and unchanging.

Very pertinent to any argument about the paleoenvironment is the overwhelming abundance of AOM within the assemblage. AOM forms from the otherwise highly labile cellular material of microbial origin, which becomes preserved in a water column that is stratified with an anoxic lower layer. This arises either because stratification reaches up into the photic zone so that microbial production becomes rapidly preserved, or because microbial remains settle down through the water column to reach the anoxic layer. There are no unequivocal marine microfossils within the samples so the palaeoenvironment was clearly not a stratified normal marine environment. This leaves open only the possibilities of a coastal back bar stratified lagoon or a depression cut into the surface of the underlying Ordovician Bighorn Dolomite or the Early Devonian Beartooth Butte Formation (Noetinger et al. 2021). In both these situations the depositional environment has to be small relative to depth or with a geometry (i.e. long and linear like a back bar lagoon) that prevents wind driven circulation that would break up the stratification. In addition, large fragments of *Archaeopteris* including small stems and leafy shoots, charcoal, and fragile reproductive structures are present on distinct bedding planes that would represent the episodic inwash of fragmentary plant remains (wrack).

The *Musivum* algae would have been growing as blooms in a 'freshwater' pool. They may represent either water derived from a nearby pool of fresh water or from within the same depositional system. The palynofacies is potentially a very significant constraint on the environmental interpretation given the abundance of *Archaeopteris* microspores and megaspores. *Archaeopteris* was a sizeable tree that has its biomass mostly within the trunk and branches (*Callixylon*) as wood, followed by its foliage. What is missing from the palynological samples is all this trunk/branch biomass as detrital debris with the *Archaeopteris* represented by its micro and megaspores and a minor component of small sized phytoclasts. The informative contrast is with the palynodebris from Carboniferous coals swamps that are dominated by plant tissue with spores being a subordinate component. This shows there was a very effective filter that only allowed an abundance of the microspores together with the much larger and normally much rarer megaspores to reach the stratified depositional environment. A plausible scenario would be that the palaeoenvironment of the *Archaeopteris* forest was arid, with little immediate surface runoff, so that the dispersed microspores and megaspores were transported by wind to the depositional environment. Periodically, storms would generate floods leading to substantial runoff that would bring into the depositional environment larger plant debris. Thus, branch and leaf debris from the surrounding *Archaeopteris* forest would reach the Maywood depositional system.

835

836 *Evidence from the macroflora*. The abundance of charcoal and large but degraded plant stems,
837 along with the rarity of foliage, provide important taphonomic insight on the depositional environment.
838 First, the large sizes of the plant macrorests indicate proximity of the depositional environment to the
839 plant source area. Given the arid climate that characterized the deposition of the Maywood Formation,
840 this implies that the land surface approached and intersected the water table in the vicinity of the
841 depositional basin, providing access to water for the vegetation that occupied a strip of land around its
842 margins, like in an oasis.
843 Second, the degraded state of this robust plant material – stems preserved without fine details –
844 indicates long residence time at the soil-water, sediment-water or water-atmosphere interface prior to
845 (transport and) burial. The rarity of well-preserved foliage is consistent with this interpretation, as leaves
846 (especially the relatively delicate archaeopterid leaves) would be the first plant parts to break down in
847 such conditions. Furthermore, the rounded ends of the stems and rounded shapes of the large charcoal
848 fragments suggest winnowing of floating plant material in the vicinity of a beach. Overall, the
849 association of plant material exhibiting all these preservational features with low-energy upper
850 shoreface and beach carbonates, suggests wrack accumulation along a protected strand plain. In other
851 words, the plant assemblages do not represent event deposition such as found in siliciclastic-dominated
852 fluvial, estuarine, or deltaic settings, but the relatively slow burial of reworked phytodebris. In this
853 context, the small delicate *Archaeopteris* sporangia and spore packages representing sporangial
854 contents, are also consistent with transport over short distances. On the other hand, the preservation of
855 such structures must represent random occurrences of fast burial from among much more abundant
856 such material that was produced in high quantities by the vegetation surrounding the basin, but of
857 which most was broken down or decayed in the taphonomically harsh environment and was not
858 preserved.
859
860 *Microconchids*. The dominance of the microconchid *Aculeiconchus sandbergi* Zaton et al. (2021)
861 at Cottonwood Canyon is of special note. This unusual accumulation of tube fossils was reported by
862 Sandberg (1963), who regarded them as the annelid worm *Spirorbis* sp. Sandberg not only noted their
863 importance in this deposit but also their association with abundant macrofloral and spore material, and
864 fragmentary fish remains. He inferred from this association that the depositional environment was
865 marginal marine but did not elaborate further.

Zaton et al. (2021) described this material from Cottonwood Canyon in detail, erecting a new genus and species (*Aculeiconchus sandbergi),* ascribing this tube fossil to the Order Microconchida within the Tentaculita, a problematic class within the lophophorates (Zaton et al. 2021; Vinn and Zaton 2012). Although the microconchids can take on a variety of growth forms (Vinn 2010), they are nonetheless obligate hard substrate encrusters. Since the Early Devonian, land plants have been one of the preferred hard surfaces occupied by microconchids (Caruso and Tomescu 2012; Matsunaga and Tomescu 2017), continuing throughout the remainder of the Paleozoic and into the Middle Triassic (Kelber 1986, 1987). Although the new microconchid *Aculeiconchus sandbergi* has not yet been observed encrusting any plant material in the Maywood Formation (Zaton et al. 2021; this study), it possesses a unique morphology of spines with flaring tips that would have acted as stilts or struts, either adding extra support to the tube on the substrate or potentially elevating it above the substrate. Although this morphology is unique among microconchids (Zaton et al. 2021), *A. sandbergi* were still clearly encrusting some hard substrate. While colonization of the water bottom is certainly a possibility, the typical microconchid substrate available in the Maywood deposit would have been plants, either the land plants preserved in the deposit or potentially aquatic primary producers (i.e., algae) not preserved in the deposit. As noted previously, the paucity of foliage among the macrofossils and the abundant abraded stem material indicates that any land plant material that entered the aquatic environment and been encrusted by microconchids would have shed these tubes through time as the plants decayed.

The co-occurrence of microconchids and land plants, often to the exclusion of any clearly marine fauna, led many researchers to the notion that microconchids in these cases represented fully freshwater environments (Caruso and Tomescu 2012; Zaton et al. 2012). This notion has not been without challenge (Gierlowski-Kordesch and Cassle 2015; see also Zaton et al. 2016 and Gierlowski-Kordesch et al. 2016), and it is here acknowledged that deposits of abundant microconchids should not be taken as *prima facie* evidence of a freshwater system. What is of interest here is that the microconchids appear to be the only skeletal invertebrates present in the deposit. This extreme dominance-low diversity community structure is indicative of a highly stressed aquatic system (Davis and Fitzgerald 2020). Stable salinity profiles, either marine or fresh water, tend to support more diverse benthic communities, while variable salinity systems tend to support only benthic organisms that can tolerate salinity stress. The salinity in the reaches of this small system may have been highly variable, driven by either seasonal evaporation/rainfall or intermittent connection to open marine waters. However, the lack of any diagnostic marine palynomorphs in these samples argues against any connection to the Maywood–Souris River marine basin to the north. Beyond salinity, the preservation of

organics and abundance of pyrite in these beds indicate that bottom-water oxygenation was reduced, also potentially limiting a more diverse benthic fauna. While the mechanism driving this oxygen stress is not known, thermal or salinity stratification in low energy systems with minimal mixing may have been important drivers (Barnes 2001).

*The weight of convergent evidence*. Taken together, the lines of evidence discussed above converge on the interpretation of the Maywood Formation in Cottonwood Canyon as the product of an isolated lagoon or lake margin depositional system. Lagoons are usually developed in arid to semi-arid climates with highly seasonal or minimal overland riverine input to the lagoon and limited connectivity to the open ocean (Davis and Fitzgerald 2020). This setting is consistent with Mid and Late Devonian paleoclimate reconstructions, which place the northern Wyoming region in the southern arid belt (Scotese 2014). As noted earlier, the Maywood Formation at Cottonwood Canyon displays no facies indicative of fluvial channel, floodplain, or fluvial-estuarine deposition. Concurrently, the Cottonwood Canyon section is far from the open, shallow marine Maywood Formation facies belt in southern Montana, thus any barriers developed at the mouth of the Beartooth Butte – Maywood valley system would have restricted marine communication to the headwaters of the valley. The lack of clearly tidal depositional features at Cottonwood Canyon, along with the thin accumulation of low-energy, wave-dominated facies indicate this was a small-fetch system with limited to no tidal communication to the open marine realm. The presence of the sarcopterygian fish *Holoptychius* also lends support to the interpretation of a freshwater depositional environment. Zaton et al. (2021) interpreted the Maywood in Cottonwood Canyon as an estuarine incised valley system, but without noting any typically fluvial-estuarine, tidal-estuarine, or marine-estuary mouth features diagnostic of this interpretation. The restricted microconchid fauna in this isolated lagoon or lake appears to have thrived in the restricted conditions, opportunistically encrusting the transported plant material and filter feeding from the nutrient-laden water. The modest wave energy transported the plants and skeletal material shoreward where it built skeletal shore berms and accumulated wrack along the margin of the lagoon.

## Conclusions

This is the first detailed account of the Maywood Formation flora, one of only three Devonian floras previously recognized in western North America. Analysis of the palynomorph and plant meso- and macrofossil content of the unit, along with observations on the fossil fauna, provide data that have implications for the age and depositional environments of the Maywood Formation, and for Devonian

vegetation and plant biogeography. The flora is heavily dominated by archaeopterid progymnosperms. The palynological assemblage lacks unequivocally marine components and supports an early Frasnian age. Vitrinite reflectivity values indicate low burial depth and temperature (c. 53°C) of the Maywood Formation. The palynomorph content, along with macro- and mesofossils including charcoal, adpressions, sporangia, and spore packages reflect a vegetation that experienced high wildfire incidence, with quasi-monodominant archaeopterids but also including the parent plant of the seed-megaspore *Spermasporites* (for which the Cottonwood Canyon occurrence represents a geographic range extension). Scales indicate the presence of sarcopterygian and tetrapodomorph fishes. Sedimentary facies, palynofacies, and plant macrofossil taphonomy are consistent with a lagoon or lake margin environment on a carbonate platform, disconnected from the open marine realm. We conclude that the arid carbonate platform of the western margin of early Frasnian Laurentia hosted a fire-prone vegetation cover dominated by archaeopterid progymnosperms. The Maywood Formation preserves fossil assemblages reflecting this vegetation at Cottonwood Canyon (Wyoming), in lagoonal or lacustrine deposits that also host microconchid tubeworms and fish. The parent plant of the seed-megaspore *Spermasporites*, present in this vegetation, was widely distributed all across Euramerica.

## Acknowledgments

Half a century ago, Fran Hueber was collecting Devonian plant fossils high on the walls of Cottonwood Canyon, not in the Maywood Formation but in the older Beartooth Butte Formation. Fran was an intrepid field paleobotanist and a dedicated student of the Devonian vegetation. We dedicate this paper to his memory, in recognition of his distinguished career and contributions to Devonian paleobotany.

Samples for this study were collected under US Bureau of Land Management permit PA10-WY-186 to AMFT; we thank Brent H. Breithaupt, Delissa L. Minnick, and Gretchen L. Hurley (BLM Wyoming) for assistance. We are indebted to the field crews of two field seasons – Shayda Abidi, Dylan Armitage, Alexander Bippus, Emma Fryer, Rachel Klassen, David Mclean, Ashley Ortiz, Kelly Pfeiler, Glenn Shelton, and Alexa Stefanakis –, to Jorge Mondéjar-Fernández for insightful discussions on fish scales, to Rudolph Serbet for facilitating specimen loans from the University of Kansas Biodiversity Institute collections, and to Candela Blanco Moreno for collection management assistance. JEAM thanks Shir Akbari for preparing the palynological samples. This study was funded in part by US National Science Foundation Graduate Research Fellowship (1546593) to Alexander Bippus, and in part by grants to AMFT from the Humboldt

State University Office of Research and Graduate Studies, Humboldt State University Sponsored Programs Foundation, and the American Philosophical Society.

## Author contributions

Field work and collection: PFH, KKSM, AMFT, and AWB. Data collection and analysis: PFH, regional geology, stratigraphy, sedimentology; JEAM, palynology; SREA and AMFT, plant macrofossils; AWB, fauna. Writing: JEAM, PFH, AMFT, AWB. All authors edited the text.

## Online-only content

Appendix A1 The appendix contains supplemental figures 1-3.

971 **Literature Cited**


972 Aboussalam ZS, RT Becker 2011 The global Taghanic biocrisis (Givetian) in the eastern Anti-Atlas,
973 Morocco. Palaeogeogr Palaeoclimatol Palaeoecol 304:136-164.

974 Algeo TJ, SE Scheckler, JB Maynard 2001 Effects of the Middle to Late Devonian spread of vascular land
975 plants on weathering regimes, marine biotas, and global climate. Pages 213-236 *in* PG Gensel, eds.
976 Plants invade the land. Columbia University Press, New York.

977 Allen KC 1965 Lower and Middle Devonian spores of North and Central Vestspitsbergen. Palaeontology
978 8:687-748.

979 Allen KC 1980 A review of *in situ* Late Silurian and Devonian spores. Rev Palaeobot Palynol 29:253-270.

980 Anderson HM, N Hiller, RW Gess 1995 *Archaeopteris* (Progymnospermopsida) from the Devonian of
981 southern Africa. Bot J Linn Soc 117:305-320.

982 Arnold CA 1936 Observations on fossil plants from the Devonian of eastern North America. I. Plant
983 remains from Scaumenac Bay, Quebec. Contrib Mus Paleontol Univ Mich 5:37-48.

984 Arnold CA 1939 Observations on fossil plants from the Devonian of eastern North America. IV. Plant
985 remains from the Catskill Delta deposits of northern Pennsylvania and southern New York. Contrib
986 Mus Paleontol Univ Mich 5:271-313.

987 Avkhimovitch VI, EV Tchibrikova, TG Obukhovskaya, AM Nazarenko, VT Umnova, LG Raskatova, VN
988 Mantsurova, S Loboziak, M Streel 1993 Middle and Upper Devonian miospore zonation of Eastern
989 Europe. Bull Cent Rech Explor-Prod Elf-Aquitaine 17:79-147.

990 Balme BE 1995 Fossil in situ spores and pollen grains: an annotated catalogue. Rev Palaeobot
991 Palynol 87:81-323.

992 Balme BE 1962 Upper Devonian (Frasnian) spores from the Carnarvon Basin, Western Australia.
993 Palaeobotanist 9:1-10.

994 Barker CE, MJ Pawlewicz 1994 Calculation of vitrinite reflectance from thermal histories and peak
995 temperatures: a comparison of methods. ACS Symp Ser Am Chem Soc 570:216-229.

996 Barnes RSK 2001 Lagoons. Pages 1427-1438 *in* JH Steele, SA Thorpe, KK Turekian, eds. Encyclopedia of
997 ocean sciences. Academc Press, San Diego.

998 Batten DJ 1996 Colonial Chlorococcales (Chapter 7C). Pages 191-203 *in* J Jansonius, DC McGregor, eds.
999 Palynology: principles and applications. American Association of Stratigraphic Palynologists, Tulsa.

1000 Beck CB 1963 *Ginkgophyton* (*Psygmophyllum*) with a stem of gymnospermic structure. Science 141:431-
1001 433.

1002 Beck CB 1970. Problems of generic delimitation in paleobotany. The genus: a basic concept in
1003 paleontology. Proc N Am Paleontol Conv 1969, Part C:173-193.
1004 Becker G, MJM Bless, M Streel, J Thorez 1974 Palynology and ostracode distribution in the Upper
1005 Devonian and basal Dinantian of Belgium and their dependence on sedimentary facies.
1006 Meded Rijks Geol Dienst 25:1-100.
1007 Benca JP, MH Carlisle, S Bergen, CAE Stromberg 2014 Applying morphometrics to early land plant
1008 systematics: a new *Leclercqia* (Lycopsida) species from Washington State, USA. Am J Bot
1009 101:510-520.
1010 Benson AL 1966 Devonian stratigraphy of western Wyoming and adjacent areas. AAPG Bull 50:2566-
1011 2603.
1012 Berner RA 1985 Sulphate reduction, organic matter decomposition and pyrite formation. Phil
1013 Trans R Soc Lond A 315:25-38.
1014 Berry CM, JEA Marshall 2015 Lycopsid forests in the early Late Devonian paleoequatorial zone of
1015 Svalbard. Geology 43:1043-1046.
1016 Braman DR, LV Hills 1992 Upper Devonian and Lower Carboniferous miospores, western District of
1017 Mackenzie and Yukon Territory, Canada. Palaeontogr Can 8:1-97.
1018 Brideaux WW, NW Radforth 1970 Upper Devonian miospores from the Escuminac Formation,
1019 eastern Quebec, Canada. Can J Earth Sci 7:29-45.
1020 Bridge JS 2006 Fluvial facies models: recent developments. Pages 85-170 *in* HW Posamentier, RG
1021 Walker, eds. Facies models revisited. SEPM Society for Sedimentary Geology, Broken Arrow.
1022 Canright JE 1970 Spores and associated macrofossils from the Devonian of Arizona. Geoscience and Man
1023 1:83-88.
1024 Caruso JA, AMF Tomescu 2012 Microconchid encrusters colonizing land plants: the earliest North
1025 American record from the Early Devonian of Wyoming, USA. Lethaia 45:490-494.
1026 Chibrikova EV 1959 Spores from the Devonian and older rocks from Bashkiria. Academy of
1027 Sciences of USSR, Bashkir Branch, Data on palaeontology and stratigraphy of Devonian and
1028 older deposits of Bashkiria:3-116 (in Russian).
1029 Chibrikova EV 1962 Spores of Devonian terrestrial deposits from Eastern Bashkiria and eastern
1030 part of Southern Urals. Academy of Sciences of USSR, Brachiopods, ostracods and spores of
1031 Middle and Upper Devonian from Bashkiria:351–476 (in Russian).

1032 Chitaley S, DC McGregor 1988 *Bisporangiostrobus harrisii* gen. et sp. nov., an eligulate lycopsid cone
1033 with *Duosporites* megaspores and *Geminospora* microspores from the Upper Devonian of
1034 Pennsylvania, U.S.A. Palaeontogr B 210:127-149.
1035 Cloutier R, S Loboziak, A-M Candilier, A Blieck 1996 Biostratigraphy of the Upper Devonian Escuminac
1036 Formation, eastern Quebec, Canada: a comparative study based on miospores and fishes. Rev
1037 Palaeobot Palynol 93:191-215.
1038 Davis RA, DM Fitzgerald 2020 Beaches and coasts. Wiley, Hoboken.
1039 Day J, BJ Witzke 2017 Upper Devonian biostratigraphy, event stratigraphy, and Late Frasnian
1040 Kellwasser extinction bioevents in the Iowa Basin, western Euramerica. Stratigraphy and
1041 Timescales 2:243-230.
1042 Day J, J Luczaj, R Anderson 2006 New perspectives and advances in understanding of Lower and
1043 Middle Paleozoic epeiric carbonate depositional systems of the Iowa and Illinois Basins.
1044 Iowa Geological Survey Guidebook 26:1-168.
1045 Dow VE 1960 Some notes on the occurrence of a coal seam in the Cedar Valley Formation of
1046 Johnson County, Iowa. Proc Iowa Acad Sci 67:253-259.
1047 Dunham RJ 1962 Classification of carbonate rocks according to depositional texture. Pages 108-121 *in*
1048 WE Ham, ed. Classification of carbonate rocks. American Association of Petroleum Geologists,
1049 Tulsa.
1050 Fairon-Demaret M, I Leponce, M Streel 2001 *Archaeopteris* from the Upper Famennian of
1051 Belgium: heterospory, nomenclature, and palaeobiogeography. Rev Palaeobot Palynol
1052 115:79-97.
1053 Gierlowski-Kordesch EH, CF Cassle 2015. The '*Spirorbis*' problem revisited: sedimentology and
1054 biology of microconchids in marine-nonmarine transitions. Earth-Sci Rev 148:209-227.
1055 Gierlowski-Kordesch EH, HJ Falcon-Lang, CF Cassle 2016 Reply to comment on the paper of
1056 Gierlowski-Kordesch and Cassle "The '*Spirorbis*' problem revisited: sedimentology and
1057 biology of microconchids in marine-nonmarine transitions" [Earth-Science Reviews, 148
1058 (2015): 209–227]. Earth-Sci Rev 152:201-204.
1059 Giesen P, CM Berry 2013 Reconstruction and growth of the early tree *Calamophyton*
1060 (Pseudosporochnales, Cladoxylopsida) based on exceptionally complete specimens from Lindlar,
1061 Germany (mid-Devonian): organic connection of *Calamophyton* branches and *Duisbergia* trunks.
1062 Int J Plant Sci 174:665-686.

1063 Glasspool IJ 2003 A review of Permian Gondwana megaspores, with particular emphasis on material
1064 collected from coals of the Witbank Basin of South Africa and the Sydney Basin of Australia. Rev
1065 Palaeobot Palynol 124:227-296.
1066 Grader GW, CM Dehler 1999 Devonian stratigraphy in east-central Idaho: new perspectives from the
1067 Lemhi Range and Bayhorse area. Pages 29-54 *in* SS Hughes, GD Thackray, eds. Guidebook to the
1068 geology of Eastern Idaho. Idaho Museum of Natural History, Pocatello.
1069 Guennel GK 1963 Devonian spores in a Middle Silurian reef. Grana 4:245-261.
1070 Hammond SE, CM Berry 2005 A new species of *Tetraxylopteris* (Aneurophytales) from the Devonian of
1071 Venezuela. Bot J Linn Soc 148:275-303.
1072 Hillier SJ, JEA Marshall 1988 A rapid technique to make polished thin sections of sedimentary organic
1073 matter concentrates. J Sediment Petrol 58:754-5.
1074 Høeg OA 1942 The Downtonian and Devonian flora of Spitsbergen. Norges Svalbard-og Ishavs-
1075 Undersøkelser 83:1-229.
1076 Hoffman MH 2020 The Devonian sedimentary record of Montana. Montana Bureau of Mines and
1077 Geology Special Publication 122:1-51.
1078 Inden RF, CH Moore 1983 Beaches. Pages 221-266 *in* P Scholle, D Bebout, C Moore, eds. Carbonate
1079 depositional environments. AAPG Memoir 33. American Association of Petroleum Geologists,
1080 Tulsa.
1081 Johnson JG, CA Sandberg, FG Poole 1988. Early and Middle Devonian paleogeography of the western
1082 United States. Pages 161-182 *in* NJ McMillan, AF Embry, DJ Glass, eds. Devonian of the world.
1083 Proceedings of the Second International Symposium on the Devonian System. Vol 1. Regional
1084 syntheses. Canadian Society of Petroleum Geologists, Calgary.
1085 Kelber K-P 1986 Taphonomische Konsequenzen aus der Besiedelung terrestrischer Pflanzen durch
1086 Spirorbidae (Annelida, Polychaete). Cour Forsch Inst Senckenberg 86:13-26.
1087 Kelber K-P 1987 Spirorbidae (Polychaeta, Sedentaria) auf Pflanzen des Unteren Keupers – Ein Beitrag zur
1088 Phyto-Taphonomie. N Jb Geol Paläont Abh 175:261-294.
1089 Knell SJ 2012 The great fossil enigma: the search for the conodont animal. Indiana University Press,
1090 Bloomington.
1091 Kräusel R, H Weyland 1941 Pflanzenreste aus dem Devon von Nord-Amerika. Palaeontogr B 86:1-78.
1092 Marshall JEA 1985 *Insculptospora*, a new genus of Devonian camerate spore with a sculptured intexine.
1093 Pollen Spores 27:453-470.

1094 Marshall JEA 1996 *Rhabdosporites langii*, *Geminospora lemurata* and *Contagisporites optivus*: an origin
1095 for heterospory within the progymnosperms. Rev Palaeobot Palynol 93:159-189.
1096 Marshall JEA 1998 The recognition of multiple hydrocarbon generation episodes: an example from
1097 Devonian lacustrine sedimentary rocks in the Inner Moray Firth, Scotland. J Geol Soc London
1098 155:335-352.
1099 Marshall JEA, AR Hemsley 2003 A mid Devonian seed-megaspore from East Greenland and the origin of
1100 the seed plants Palaeontology 46:647-670.
1101 Marshall JEA, OP Tel'nova, CM Berry 2019 Devonian and Early Carboniferous coals and the evolution of
1102 wetlands. Vestnik IG Komi SC UB RAS 10:12-15.
1103 Marshall JEA, JF Brown, TR Astin 2011 Recognising the Taghanic crisis in the Devonian terrestrial
1104 environment; its implications for understanding land-sea interactions. Palaeogeogr
1105 Palaeoclimatol Palaeoecol 304:165-183.
1106 Marshall JEA, H-C Zhu, CH Wellman, CM Berry, Y Wang, H Xu, P Breuer 2016 Provincial Devonian spores
1107 from South China, Saudi Arabia and Australia. Rev Micropaléontol 60:403-409.
1108 Matsunaga KKS, AMF Tomescu 2017 An organismal concept for *Sengelia radicans* gen. et sp. nov. –
1109 morphology and natural history of an Early Devonian lycophyte. Ann Bot 119:1097-1113.
1110 McGregor DC 1964 Devonian miospores from the Ghost River Formation, Alberta. Bull Geoll Surv Canada
1111 109:1-31.
1112 McGregor DC 1979 Devonian miospores of North America. Palynology 3:31-52.
1113 McGregor DC 1996 Spores of the Escuminac Formation. Pages 91-102 *in* H-P Schultze, R Cloutier, eds.
1114 Devonian fishes and plants of Miguasha, Quebec, Canada. Pfeil, München.
1115 McGregor DC, M Camfield 1982 Middle Devonian miospores from the Cape De Bray, Weatherall, and
1116 Hecla Bay Formations of northeastern Melville Island, Canadian Arctic. Bull Geol Surv Canada
1117 348:1-105.
1118 McGregor DC, B Owens 1966 Illustrations of Canadian fossils: Devonian spores of eastern and
1119 northern Canada. Geol Surv Canada Paper 66-30:1-66.
1120 McMannis WJ 1962 Devonian stratigraphy between Three Forks, Montana and Yellowstone Park.
1121 Pages 4-12 *in* AR Hansen, JH McKeever, eds. Three Forks – Belt Mountains Area: the
1122 Devonian System of Montana and adjacent areas, 13th Annual Field Conference. Billings
1123 Geological Society, Billings.
1124 Meyers JH 1980 Tidal-flat carbonates of the Maywood Formation (Frasnian) and the Cambrian-
1125 Devonian unconformity, southwestern Montana. Pages 39-53 in TD Fouch, ER Magatham,

1126 eds. Paleozoic paleogeography of the western United States. SEPM Society for Sedimentary
1127 Geology, Broken Arrow.
1128 Mikesh DL 1965 Correlation of Devonian strata in northwestern Wyoming. MSc thesis. University
1129 of Iowa, Iowa City.
1130 Mondéjar-Fernández J, G Clément 2012 Squamation and scale microstructure evolution in the
1131 Porolepiformes (Sarcopterygii, Dipnomorpha) based on *Heimenia ensis* from the Devonian of
1132 Spitsbergen. J Vertebr Paleontol 32:267-284.
1133 Mondéjar Fernández J, FJ Meunier 2021 New histological information on *Holoptychius* Agassiz, 1839
1134 (Sarcopterygii, Porolepiformes) provides insights into the palaeoecological implications and
1135 evolution of the basal plate of the scales of osteichthyans. Hist Biol 33:2276-2288.
1136 Mondéjar-Fernández J, P Janvier 2021 Finned vertebrates. Pages 294-324 *in* V de Buffrénil, AJ de Ricqlès,
1137 L Zylberberg, K Padian, eds. Vertebrate skeletal histology and paleohistology. Routledge, New
1138 York.
1139 Naumova SN 1953 Upper Devonian spore-pollen assemblages of the Russian Platform and their
1140 stratigraphic significance. Transactions of the Institute of Geological Sciences, Academy of
1141 Sciences of the USSR 143 (Geological Series no. 60):1-204 (in Russian).
1142 Noetinger S, AC Bippus, AMF Tomescu 2021 Palynology of a short sequence of the Lower Devonian
1143 Beartooth Butte Formation at Cottonwood Canyon (Wyoming): age, depositional environments
1144 and plant diversity. Pap Palaeontol 7: 2183-2204.
1145 Orlova OA, AL Jurina, SM Snigirevsky 2016 Late Devonian plant communities of North Russia. Rev
1146 Palaeobot Palynol 224:94-107.
1147 Owens B 1971 Miospores from the Middle and early Upper Devonian rocks of the Western Queen
1148 Elizabeth Islands, Arctic Archipelago. Geol Surv Canada Paper 70-38:1-157.
1149 Peppers RA, HH Damberger 1969 Palynology and petrography of a Middle Devonian coal in Illinois.
1150 Illinois State Geological Survey Circular 445:1-35.
1151 Pettitt JM 1965 Two heterosporous plants from the Upper Devonian of North America. Bull Br Mus (Nat
1152 Hist) 10:83-92.
1153 Pettitt JM 1966 Exine structure in some fossil and Recent spores and pollen as revealed by light and
1154 electron microscopy. Bull Br Mus (Nat Hist) 13:223-257.
1155 Phillips TL, HN Andrews, PG Gensel 1972 Two heterosporous species of *Archaeopteris* from the Upper
1156 Devonian of West Virginia. Palaeontogr B 139:47-71.

1157 Playford G 1983 The Devonian miospore genus *Geminospora* Balme, 1962 a reappraisal based upon
1158 topotypic *G. lemurata* (type species). Mem Assoc Australas Palaeontol 1:311-325.

1159 Playford G 1993 Miospores and organic-walled microphytoplankton characteristic of strata contiguous
1160 with the Devonian-Carboniferous boundary. Comptes rendus, 12th International Congress on the
1161 Carboniferous and Permian (1991) 1:127-160.

1162 Playford G, R Wicander, GD Wood 1983 *Laiphospora*, a new genus of trilete *sporae dispersae* from the
1163 Devonian of North America. Palynology 7:211-219.
1164 Potonié R 1956 Synopsis der Gattungen der Sporae dispersae, 1. Teil: *Sporites*. Beih Geol Jahrb 23:1-103.
1165 Potonié R 1958 Synopsis der Gattungen der Sporae dispersae, 2. Teil: *Sporites* (nachträge), *Saccites*,
1166 *Aletes*, *Praecolpates*, *Polyplicates*, *Monocolpates*. Beih Geol Jahrb 31:1-114.
1167 Richardson JB 1965 Middle Old Red Sandstone spore assemblages from the Orcadian basin, north-
1168 east Scotland. Palaeontology 7:559-605.
1169 Richardson JB, DC McGregor 1986 Silurian and Devonian spore zones of the Old Red Sandstone
1170 Continent. Geol Surv Canada Bull 364:1-79.
1171 Riegel W 1973 Sporenformen aus den Heisdorf-, Lauch- und Nohn-Schichten (Emsium und Eifelium) der
1172 Eifel, Rheinland. Palaeontogr B 142:78-104.
1173 Riegel W 1974 Spore floras across the Lower/Middle Devonian boundary in the Rhineland (G.R.F.). Pages
1174 47-52 *in* Palynology of the Proterophyte and Palaeophyte. Proceeding of the 3rd International
1175 Palynological Conference (1971). Academy of Sciences of the USSR, Geological Institute, Moscow.
1176 Sandberg, CA 1961a Distribution and thickness of Devonian rocks in Williston Basin and in central
1177 Montana and north-central Wyoming. Bull US Geol Surv 1112-D:105-127.
1178 Sandberg CA 1961b Widespread Beartooth Butte Formation of Early Devonian age in Montana and
1179 Wyoming and its paleogeographic significance. AAPG Bull 45:1301-1309.
1180 Sandberg CA 1963 Spirorbal limestone in the Souris River(?) Formation of Late Devonian Age at
1181 Cottonwood Canyon, Bighorn Mountains, Wyoming. U.S. Geol Surv Prof Paper 63:C14-C16.
1182 Sandberg CA 1967 Measured sections of Devonian rocks in northern Wyoming. Geological Survey of
1183 Wyoming Bull 52. University of Wyoming, Laramie.
1184 Sandberg CA, WJ McMannis 1964 Occurrence and paleogeographic significance of the Maywood
1185 Formation of Late Devonian age in the Gallatin Range, southwestern Montana. US Geol Surv Prof
1186 Paper 501-C:C50-C54.
1187 Sandberg CA, RC Gutschick, JG Johnson, FG Poole, WJ Sando 1982 Middle Devonian to Late Mississippian

1188 geologic history of the Overthrust Belt region, western United States. Pages 691-719 *in* RB Powers,
1189 ed. Geologic studies of the Cordilleran thrust belt. Vol 2. Rocky Mountain Association of Geologists
1190 Denver.
1191 Sanders RB 1968 Devonian spores of the Cedar Valley Coal of Iowa, U.S.A. Jour Palynol 2:16-32.
1192 Schultze HP 2016 Scales, enamel, cosmine, ganoine, and early osteichthyans. C R Palevol 15:87-106.
1193 Scotese CR 2014 Atlas of Devonian paleogeographic maps. PALEOMAP atlas for ArcGIS. Vol 4, The Late
1194 Paleozoic, Maps 65-72, Mollweide Projection. PALEOMAP Project, Evanston.
1195 Selwood EB, JM Thomas, GD Borley, A Dean 1993 A revision of the Upper Palaeozoic stratigraphy
1196 of the Trevone Basin, north Cornwall, and its regional significance. Proc Geol Assoc 104:137-
1197 148.
1198 Stein WE, F Mannolini, LV Hernick, E Landing, CM Berry 2007 Giant cladoxylopsid trees resolve the
1199 enigma of the Earth's earliest forest stumps at Gilboa. Nature 46: 904-907.
1200 Stein WE, CM Berry, LV Hernick, F Mannolini 2012 Surprisingly complex community discovered in
1201 the mid-Devonian fossil forest at Gilboa. Nature 483:78-81.
1202 Stein WE, CM Berry, JL Morris, LV Hernick, F Mannolini, C Ver Straeten, E Landing, JEA Marshall, CH
1203 Wellman, DJ Beerling, JR Leake 2019 Mid-Devonian *Archaeopteris* roots signal revolutionary
1204 change in earliest fossil forests. Curr Biol 30:1-11.
1205 Stockmans F 1968 Végétaux mésodévoniens récoltés aux confins du Massif du Brabant (Belgique). Mem
1206 Inst R Sci Nat Belg 159:1-49.
1207 Stockmans F, Y Willière 1966 Les acritarches du Dinantien du Sondage de l'asile d'aliénés à
1208 Tournai (Belgique). Bull Soc Belge Géol Paléont Hydrol 74:462-477.
1209 Stone JL 1973 Problems with the name "*Platyphyllum*".Taxon 22:105-108.
1210 Taugourdeau-Lantz J 1960 Sur la microflore du Frasnien inférieur de Beaulieu (Boulonnais). Rev
1211 Micropaléont 3:144-154.
1212 Taugourdeau-Lantz J 1967 Les spores du Frasnien du Bas-Boulonnais (France). Rev Palaeobot
1213 Palynol 1:131-139.
1214 Teichert C, JM Schopf 1958 A Middle or Lower Devonian psilophyte flora from central Arizona and
1215 its paleogeographic significance. J Geol 66:208-217.
1216 Turnau E, G Racki 1999 Givetian palynostratigraphy and palynofacies: new data from the Bodzentyn
1217 Syncline (Holy Cross Mountains, central Poland). Rev Palaeobot Palynol 106:237-271.
1218 Tyson RV 1995 Sedimentary organic matter. Chapman & Hall, London.

1219 Vigran JO 1964 Spores from Devonian deposits, Mimerdalen, Spitsbergen. Norsk Polarinst Skr Nr
1220 132:1-32.
1221 Vinn O 2010 Adaptive strategies in the evolution of encrusting tentaculitoid tubeworms.
1222 Palaeogeogr Palaeoclimatol Palaeoecol 292:211-221.
1223 Vinn O, M Zaton 2012 Phenetic phylogenetics of tentaculitoids – extinct, problematic calcareous
1224 tube-forming organisms. Geol Fören Stockh Förh 134:145-156.
1225 Wicander R, G Playford 1985 Acritarchs and spores from the Upper Devonian Lime Creek
1226 Formation, Iowa, U.S.A. Micropalaeontology 31:97-138.
1227 Witzke BJ, BJ Bunker 2006 Stratigraphy of the Wapsipinicon Group (Middle Devonian) in
1228 southeastern Iowa. Iowa Geological Survey Guidebook 26:47-58.
1229 Wood GD, E Turnau 2001 New Devonian coenobial Chlorococcales (Hydrodictyaceae) from the
1230 Holy Cross Mountains and Radom-Lublin region of Poland: their paleoenvironmental and
1231 sequence stratigraphic implications. Pages 53-63 *in* DK Goodman, RT Clarke, eds.
1232 Proceedings of the 9th International Palynological Congress (1996). American Association of
1233 Stratigraphic Palynologists, Houston.
1234 Zaton M, O Vinn, AMF Tomescu 2012 Invasion of freshwater and variable marginal marine
1235 habitats by microconchid tubeworms – an evolutionary perspective. Geobios 45:603-610.
1236 Zaton M, MA Wilson, O Vinn 2016 Comment on the paper of Gierlowski-Kordesch and Cassle "The
1237 '*Spirorbis*' problem revisited: sedimentology and biology of microconchids in marine-
1238 nonmarine transitions" [Earth-Science Reviews, 148 (2015): 209–227]. Earth-Sci Rev
1239 152:198-200.
1240 Zaton M, M Hu, M di Pasquo, PM Myrow 2021 Adaptive function and phylogenetic significance of
1241 novel skeletal features of a new Devonian microconchid tubeworm (Tentaculita) from
1242 Wyoming, U.S.A. J Paleont. doi: 10.1017/jpa.2021.71.

**Figure captions**

**Fig. 1** Base map of the Cottonwood Canyon study area. The locality is on the northwest flank of the Bighorn Mountains, c. 27 km east of Lovell, Big Horn County, Wyoming (44° 52'14.08" N, 108° 3' 26.21" W). The 1500-meter contour roughly delineates the base of the steep western edge of the Bighorn Mountains. The section is 1.16 km from the Cottonwood Canyon trailhead along the trail following Cottonwood Creek, plus 150 m north of the trail, on the north wall of Cottonwood Canyon. The trailhead is located at the end of Cottonwood Canyon Road c. 9 km from the junction with Alternate US Route 14.

**Fig. 2** Chronostratigraphic chart of Lower and Middle Paleozoic units exposed in Cottonwood Canyon. Formations and their age are indicated, vertical lines indicate gaps with no rock record. The Cambrian Gallatin Group, Upper Ordovician Bighorn Dolomite, and Upper Devonian Jefferson Formation are found throughout Cottonwood Canyon. The Beartooth Butte and Maywood Formations are only found in isolated exposures where they have truncated into the underlying Bighorn Dolomite. Note that most of Ordovician, Silurian, and Devonian time is not recorded in Cottonwood Canyon strata.

**Fig. 3** Paleogeography of the Maywood and Souris River Formations in Montana and northern Wyoming (after Hoffman 2020). Thick and shallow marine facies (blue) of the Maywood Formation in western Montana and the Souris River Formation in the Williston Basin of eastern Montana are mapped as thinning wedges onlapping the extended Transcontinental Arch in central Montana (ancestral Central Montana Uplift) and southward into Wyoming. A transition zone of thin, discontinuous outcrops of age-equivalent continental strata (green) are recognized in outcrops from southwestern Montana and the Bighorn Mountains of northern Wyoming, and are here considered Maywood Formation; position of studied section indicated by red triangle.

**Fig. 4** *A*, Stratigraphic column of the Maywood Formation at the study site in Cottonwood Canyon (Wyoming). This thin formation is underlain by the Upper Ordovician Bighorn Dolomite and overlain by the Late Devonian Jefferson Formation. Gross lithologies of the Maywood Formation include dolostone, dolomitic limestone, and limestone with a thin parting of calcareous shale. Carbonate textures range from mudstones to grainstones (after Dunham 1962). Planar laminations dominate the sedimentary bedding structures, although ripple and longer wavelength wavy laminations are also present. Carbonate grain components include peloids and skeletal material. Skeletal elements appear to be

exclusively of the microconchid *Aculeiconchus sandbergi* Zaton et al. 2021. Non-carbonate material includes phytodebris (plant compressions and charcoal) and vertebrate fragments. Palynology samples (P1-P26) indicated by green arrowheads. *B*, Log of abundances of *Archaeopteris* megaspores per gram of sediment. *C*, relative percentages of *Geminospora lemurata* in the microspore assemblage.

**Fig. 5** *Archaeopteris* micro- and megaspores from the Maywood Formation in Cottonwood Canyon (Wyoming). Sample and slide numbers are given; coordinates (e.g., 120.2, 6.6) are for Olympus BHS-313 microscope No. 230272 in the School of Ocean and Earth Sciences, University of Southampton together with the slides for the figured specimens; England Finder references are given e.g., E38/3. *A-H*, *Geminospora lemurata*. *A*, SR-5; 138.1, 21.7; E38/3. *B*, SR-5; 134.4, 22.2; E34/1. *C*, SR-5; 131, 21.5; P30/2. *D*, SR-5; 138.1, 20.2; G38/1. *E*, SR-5; 136, 21.6; E36, 3. *F*, SR-5; 131.6, 13.7; N31/3. *G*, SR-5; 134.8, 22.4; D34/4. *H*, SR-5; 132.5, 16.1; X36/1. *I-K*. *Contagisporites optivus*. *I*, SR-14 mega oxid; 136, 4.6; X36/1. *J*, SR-15 mega oxid 1; 109.7, 12.7; P8/2. *K*, SR-15 mega 130, 18.8; H29/4. *L-M*, *Contagisporites optivus*, corroded specimens with visible intexines. *L*, SR-5 mega 1, 134.2, 13.4; O34/1. *M*, SR-9 mega 1; 112, 3.7; Y11/1. *N-U*, *Archaeozonotriletes macromanifestus*. *N*, SR-16 mega, 122.4, 17.8; J24/3. *O*, SR-15, oxid 1; 141.8, 11.1; Q42/3. *P*, Sr-15 mega oxid 1; 121, 23.7; C20/4. *Q*, SR-13 mega; 141, 7.8; U41/1. *R*, SR-15 mega oxid; 144.9, 4.9; note sculpture typical of var. *vorobjevensis*. *S*, SR-15 mega oxid 2; 131.0, 9.0; S30/4. *T*, SR-15 mega oxid; 120.2, 6.6; V19/2. *U*, SR-14, mega oxid; 113, 10.2; R12/3. All scale bars10 µm.

**Fig. 6** Spores, prasinophyte and chlorophyte algae from the Maywood Formation in Cottonwood Canyon (Wyoming). Sample and slide numbers are given; coordinates are for Olympus BHS-313 microscope No. 230272 in the School of Ocean and Earth Sciences, University of Southampton together with the slides for the figured specimens. *A*, *Retusotriletes birealis*, SR-5; 125, 18.7. *B*, *Retusotriletes distinctus*, SR-11; 130.8, 10.9. *C*, *Retusotrilete pychovii*, SR-12; 130.2, 12.1. *D*, *Calamospora* sp., SR-5; 124.1, 20. *E*, *Aneurospora greggsii*, SR-12; 139.1, 13.9. *F*, *Rhabdosporites langii*, SR-5; 122.5, 14.7. *G*, *Laiphospora membrana*, SR-12; 131.7, 13. *H*, *I*, *Ancyrospora* sp. (*I* is enlargement of bifurcate spine tip), SR-5; 126.2, 23.9. *J*, *Anapiculatisporites petilus*, SR-2; 127, 13. *K*, *Cristatisporites cariosus*, SR-16; 122.9, 18.3. *L*, *Insculptospora incrustata*, SR-15 mega oxid 1; 134.6, 21.2. *M*, *Insculptospora confossa*, SR-6; 129.4, 7.6. *N*, *Stenozonotriletes ornatus*, SR-12; 134.8, 13.6. *O*, *Cristatisporites cariosus*, SR-16; SR-5; 123.4, 9. *P*, *Cristatisporites triangulatus*, SR-16; 121.4, 17.9. *Q*, *Musivum gradzinskii*, SR-8; 125.6, 13.1.

*R*, *Tasmanites*, SR-5 lc; 127.2, 12.2. *S*, *Lophosphaeridium*, SR-7; 124.4, 11.2. *T*, *Tornacia sarjeantii* SR-17; 130.9, 16.4. All scale bars10 µm.

**Fig. 7** Megaspore dimensions (Maywood Formation, Cottonwood Canyon, Wyoming). Cross plot of exoexine versus intexine diameters for *Contagisporites optivus* (red dots) and the larger *Archaeopteris* megaspores (*Archaeozonotriletes macromanifestus*; blue dots) separated by the possession of a curvatural ring. The plot shows a continuous distribution with a consistent ratio between exoexine and intexine diameters. The histogram based on the relative proportions of the megaspores (*Contagisporites optivus* – red; larger *Archaeozonotriletes* – blue) showing the smaller numbers of *Contagisporites* megaspores present relative to the larger more mature spores.

**Fig. 8** Macroflora of the Maywood Formation in Cottonwood Canyon (Wyoming); charcoalified material and adpressions. *A*, Large charcoalified axis on bedding plane (running bottom left to top right); the charcoal is fragmented and part of it crumbled leaving an impression; HPH710; scale 2 cm. *B*, Large wood charcoal fragment with rounded outline, flattened on a bedding plane; HPH711; scale 2 cm. *C*, Bedding plane with small evenly distributed charcoal and coalified plant fragments, and small fragments of thin axes; HPH712; scale 2 cm. *D*, View of vertical plane of fracture in the layers; note rounded wood charcoal fragments of different sizes, oriented with their long axes parallel to bedding planes; HPH713; scale 1 cm. *E*, Bedding plant with large flattened wood charcoal fragments and charred axes of different sizes; axes are compressed, often with rounded ends and their charcoal is crumbly and disaggregates leaving impressions that harbor small bits of charcoal and orthogonal lattices of fine veins formed by diagenetic mineral precipitation (arrowhead); HPH713; scale 2 cm. *F*, Bedding plane with axis fragments and amorphous plant fragments of various sizes, some charred others carbonaceous compressions and corresponding impressions; some axis fragments have rounded ends; in others, the charcoal is crumbly and disaggregates leaving impressions that harbor small bits of charcoal and orthogonal lattices of fine veins formed by diagenetic mineral precipitation (arrowhead); HPH714; scale 2 cm.

**Fig. 9** Macroflora of the Maywood Formation in Cottonwood Canyon (Wyoming); adpressions. *A*, *B*, *C*, Axes of various sizes preserved as carbonaceous compressions may be more or less oxidized, depending on the sedimentary facies of the host layer; most of the axes are non-descript short fragments that do not exhibit appendages or branching; HPH715 (*A*, scale 2 cm); HPH716 (*B*, scale 2 cm); HPH717 (*C*, scale 2 cm). *D*, A horizon that preserves a dense mat of oxidized, compressed intertwined leafy axes; HPH718;

scale 3 cm. *E*, Detail of *D*; some of the axes are split longitudinally in several places, which are similar to points of leaf dissection; HPH718; scale 2 mm. *F*, Detail of *D*; leaf bases (traced in orange, at arrowheads) are difficult to ascertain, due to the dense intertwining of axes, as well as their state of decomposition and the oxidized state of the fossil material; HPH718; scale 5 mm.

**Fig. 10** Macroflora of the Maywood Formation in Cottonwood Canyon (Wyoming); adpressions and charcoal. *A*, Dichotomously branched axis bearing irregularly-spaced bases of lateral appendages; HPH719; scale 2 cm. *B*, Thin axis with undulating habit and isotomous branching; HPH720; scale 1 cm. *C*, *D*, Fan-shaped leaves dissected into strap-shaped distal lobes with rounded margin; HPH721 (*C*, scale 2mm; *D*, scale 1 mm). *E*, Archaeopterid wood charcoal fragment in the sedimentary matrix; note fish scale (orange) under the charcoal; HPH722 slide 1; scale 1 mm. *F*, Transverse section of charcoalified archaeopterid wood; note evenly-sized tracheids and uniseriate rays (between arrowheads); HPH722 slide 2; scale 200 µm. *G*, Oblique longitudinal tangential section of charcoalified archaeopterid wood; note uniseriate rays only a few cells high (between arrowheads); HPH722 slide 3; scale 200 µm. *H*, Oblique longitudinal tangential section of charcoalified archaeopterid wood; note groups of mostly biseriate pits; HPH722 slide 4; scale 200 µm.

**Fig. 11** Flora of the Maywood Formation in Cottonwood Canyon (Wyoming); sporangia and spores. *A*, *B*, Archaeopterid sporangia with fusiform shape retrieved from rock macerates; note epidermis with long narrow cells, dehiscence line that runs the entire length of the sporangium (in *A*), and fully opened sporangium (in *B*); HPH723 (*A*, scale 200 µm); HPH724 (*B*, scale 200 µm). *C*, *D*, Clumps of archaeopterid spores (*C* – microspores; *D* – megaspores) retrieved from rock macerates, representing undissociated contents of sporangia; HPH725 (*C*, scale 200 µm); HPH726 (*D*, scale 200 µm). *E*, *F*, *G*, Isolated archaeopterid sporangia exposed on bedding planes; note fusiform shape of the sporangia and sporangium attached to sporophyll fragment (in *G*); HPH727 (*E*, scale 200 µm); HPH728 (*F*, scale 400 µm); HPH728 (*G*, scale 500 µm). *H*, Apical fragments of four sporangia probably attached to the same sporophyll; HPH718; scale 200 µm. *I*, Dense aggregation of clusters of microspores (representing undissociated contents of archaeopterid sporangia) exposed on a bedding plane; HPH729; scale 500 µm. *J*, Isolated archaeopterid megaspore (at center of image) exposed on bedding plane; HPH727; scale 400 µm. *K*, Large isolated spore reminiscent of *Ancyrospora* exposed on bedding plane; HPH712; scale 200 µm.

**Fig. 12** Flora of the Maywood Formation in Cottonwood Canyon (Wyoming); *Spermasporites*-type seed-megaspores. *A*, *B*, *C*, *D*, Specimens retrieved from rock macerates; note abortive megaspores at top of the large functional megaspore (*A* and *C*), mass of microspores around the abortive megaspores (*A*), outer wall layer covering the seed-megaspores partially (*A*) or entirely (*D*) and exhibiting characteristic longitudinal folds (*A*), and dark inner body inside the functional megaspore (in *B* and possibly *C*); HPH730 (*A*, scale 200 µm); HPH731 (*B*, scale 200 µm); HPH732 (*C*, scale 200 µm); HPH733 (*D*, scale 200 µm). *E*, Seed-megaspore or its separated external wall layer exposed on bedding plane; note longitudinal folds characteristic of the outer wall layer of seed-megaspores; HPH714; scale 500 µm. *F*, Detail of *A* showing proximal pole of functional megaspore with two sides of the trilete mark (arrowheads) and parts of the abortive megaspores (top); HPH730; scale 100 µm. *G*, Detail of *A* showing abortive megaspores (dark) surrounded by mass of microspores; HPH730; scale 100 µm. *H*, Detail of *B* showing proximal pole of functional megaspore with two sides of the trilete mark partially open (arrowheads); HPH731; scale 100 µm.

**Fig. 13** Animal fossils in the Maywood Formation at Cottonwood Canyon (Wyoming). *A*, Fragment of fish scale sectioned vertically in petrographic thin-section (detail of fig. 10*E*); note large canals forming a network underlain by a thick dense bony layer with narrow vascular canals, all reminiscent of the histology of sarcopterygian cosmoid scales; HPH722 slide 1; scale 400 µm. *B*, Isolated sarcopterygian fish scale exposed on bedding plane; note round outline with fine anteroposteriorly oriented ridges on the posterior edge (top right) and low tubercles in the anterior area (bottom left and toward center of scale), similar to tetrapodomorph scales; HPH734; scale 2 mm. *C*, *D*, Two views of elongated dark brown object deposited parallel with the bedding planes, interpreted as a coprolite; note orthogonal network of fine diagenetic mineral precipitation veins crossing the object; HPH722; scale 1 cm. *E*, *F*, Longitudinal (*E*) and transverse (*F*) section of object interpreted as coprolite; note amorphous material that forms "swirly" texture around "nests" of angular fragments, and network of fine diagenetic mineral precipitation veins; HPH722 slide 5 (*E*, scale 2 mm); HPH722 slide 6 (*F*, scale 2 mm).

**Fig. 14** Deep Time™ paleogeography map of Euramerica and northern Gondwana showing the location of the Cottonwood Canyon exposure of the Maywood Formation (red dot) at the western extremity of the Mid West carbonate platform, and previously published Mid and early Late Devonian spore assemblages from other localities on the carbonate platform and in northern Canada (blue dots).

**Table 1** Spore and microplankton – taxonomic citations

*Anapiculatisporites apiculatus* Guennel 1963

*Anapiculatisporites davenportensis* Peppers in Peppers and Damberger 1969

*Anapiculatisporites petilus* Richardson 1965

*Aneurospora greggsii* (McGregor) Becker, Bless, Streel and Thorez 1974

*Apiculatasporites wapsipiniconensis* Guennel 1963

*Archaeozonotriletes macromanifestus* Naumova 1953

*Archaeozonotriletes variabil*s Naumova 1953

*Biharisporites ellesmerensis* Chaloner 1959

*Biharisporites maguashensis* Brideaux and Radforth 1970

*Biharisporites spitsbergensis* Vigran 1964

*Contagisporites optivus* (Chibrikova) Owens 1971

*Contagisporites optivus optivus* (Chibrikova) Owens 1971

*Contagisporites optivus vorobjevensis* (Chibrikova) Owens 1971

*Cristatisporites cariosus* Wicander and Playford 1985

*Cristatisporites intermedius* Guennel 1963

*Cristatisporites triangulatus* Allen 1965

*Geminospora lemurata* (Balme) Playford 1983

*Geminospora micromanifesta* (Naumova) McGregor and Camfield 1982 var. *minor* Naumova 1953

*Insculptospora incrustata* (Arkhangelskaya) Marshall 1985

*Insculptspora confossa* (Richardson) Marshall 1985

*Laiphospora membrana* (Sanders) Playford, Wicander and Wood 1983

*Retusotriletes biarealis* McGregor 1964

*Retuotriletes pychovii* Naumova 1953

*Retusotriletes distinctus* Richardson 1965

*Rhabdosporites cuvillieri* Taugourdeau-Lantz 1967

*Rhabdosporites langii* (Eisenack) Richardson 1960

*Stenozonotriletes bellus* Guennel 1963

*Stenozonotriletes ornatus* Naumova 1953

*Verrucosisporites ellesmerensis* (Chaloner) Chi and Hills 1976

*Veryhachium octoaster* Staplin 1961

*Musivum gradzinskii* Wood and Turnau 2001

*Tornacia sarjeantii* Stockmans and Willière 1966

Figure 1

Click here to access/download;Figure;Figure1.tif

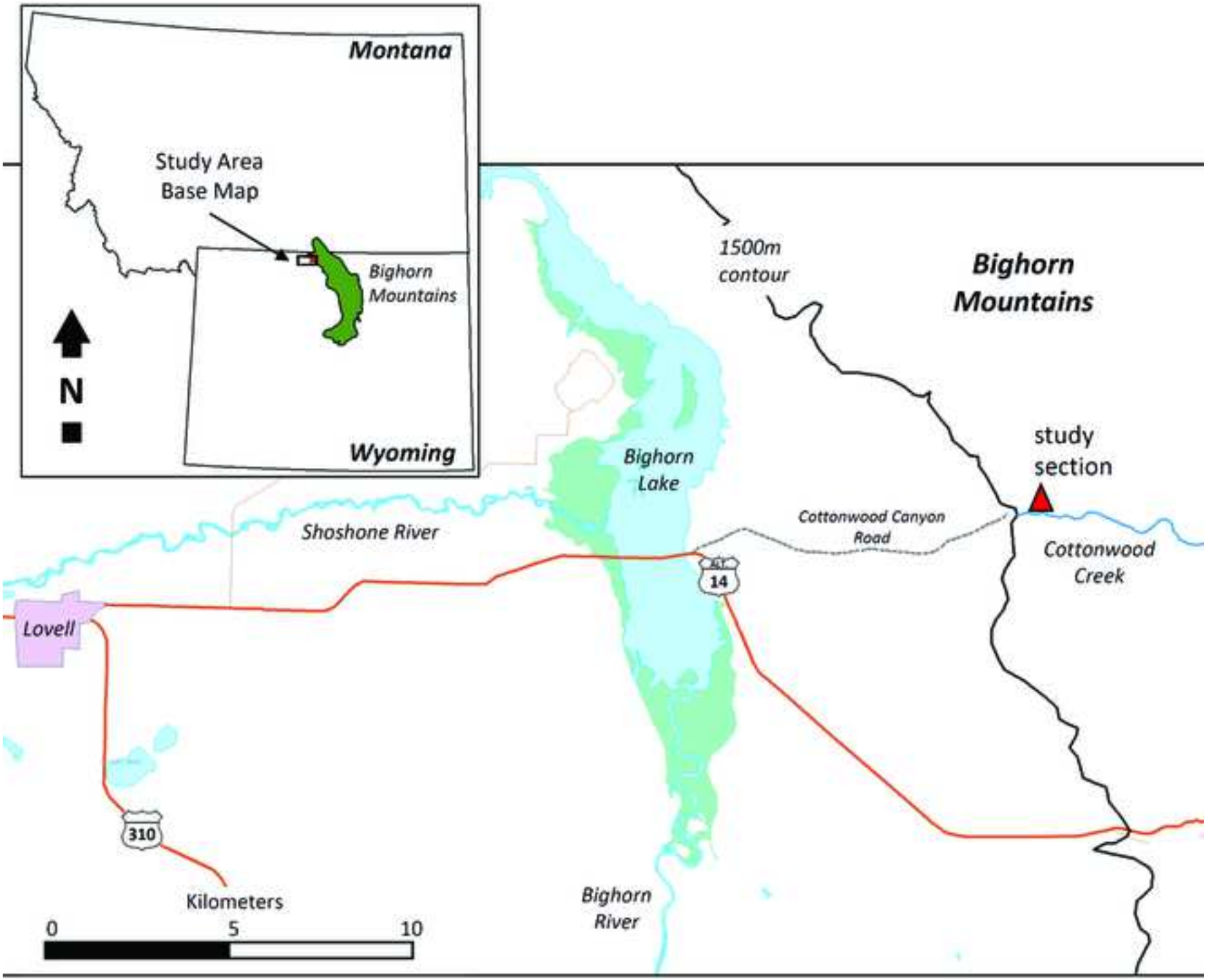

Figure 2



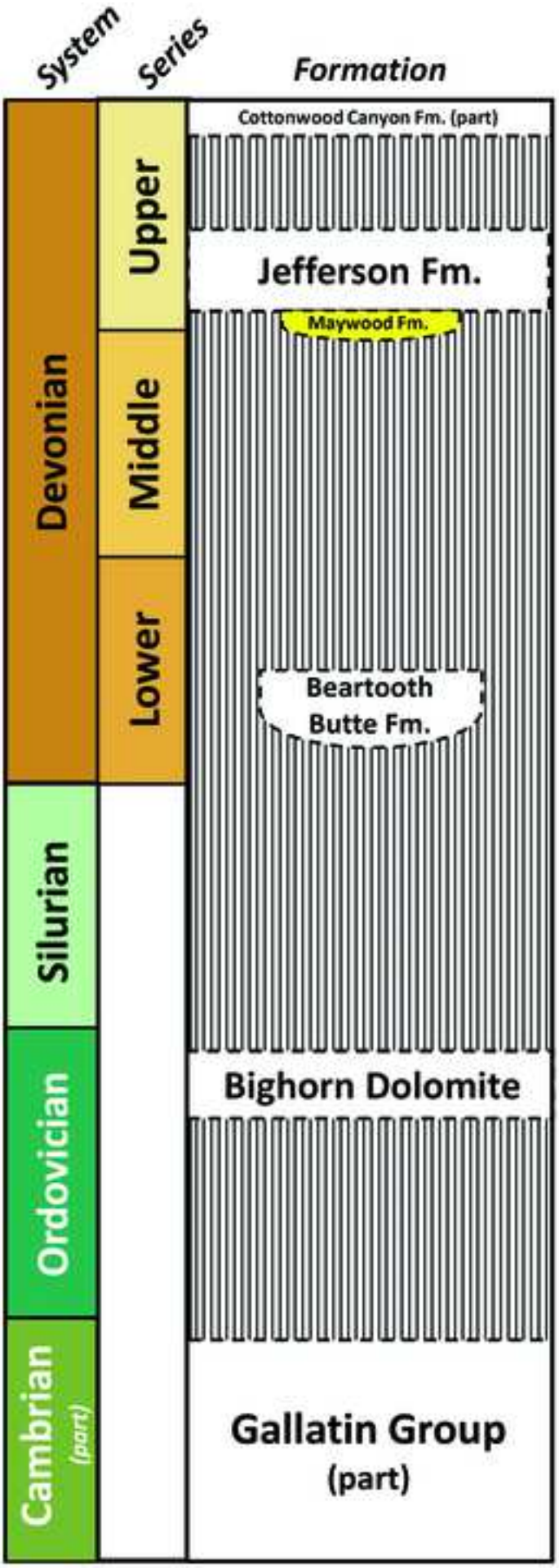

Figure 3

Click here to access/download;Figure;Figure3.tif

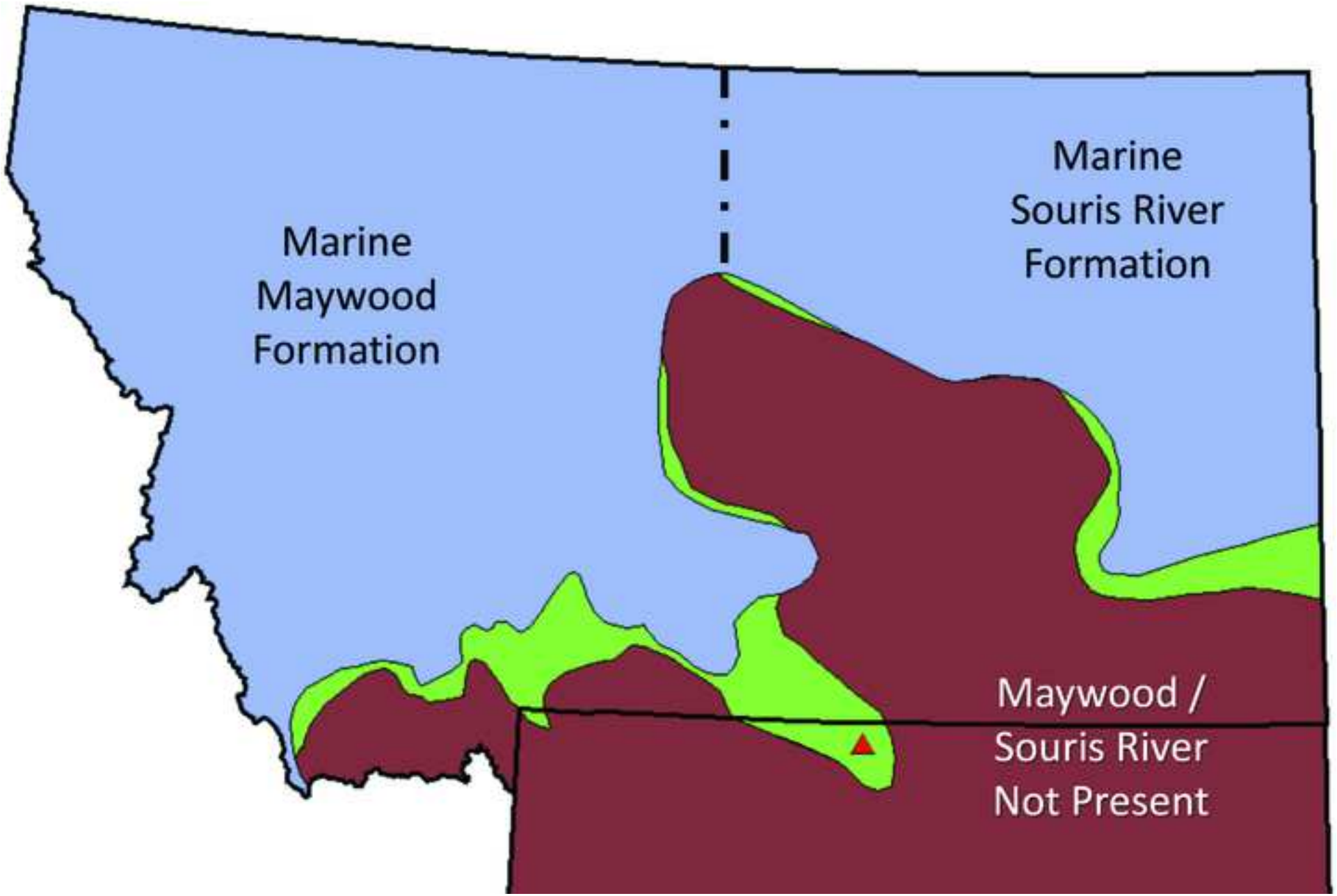

Figure 4



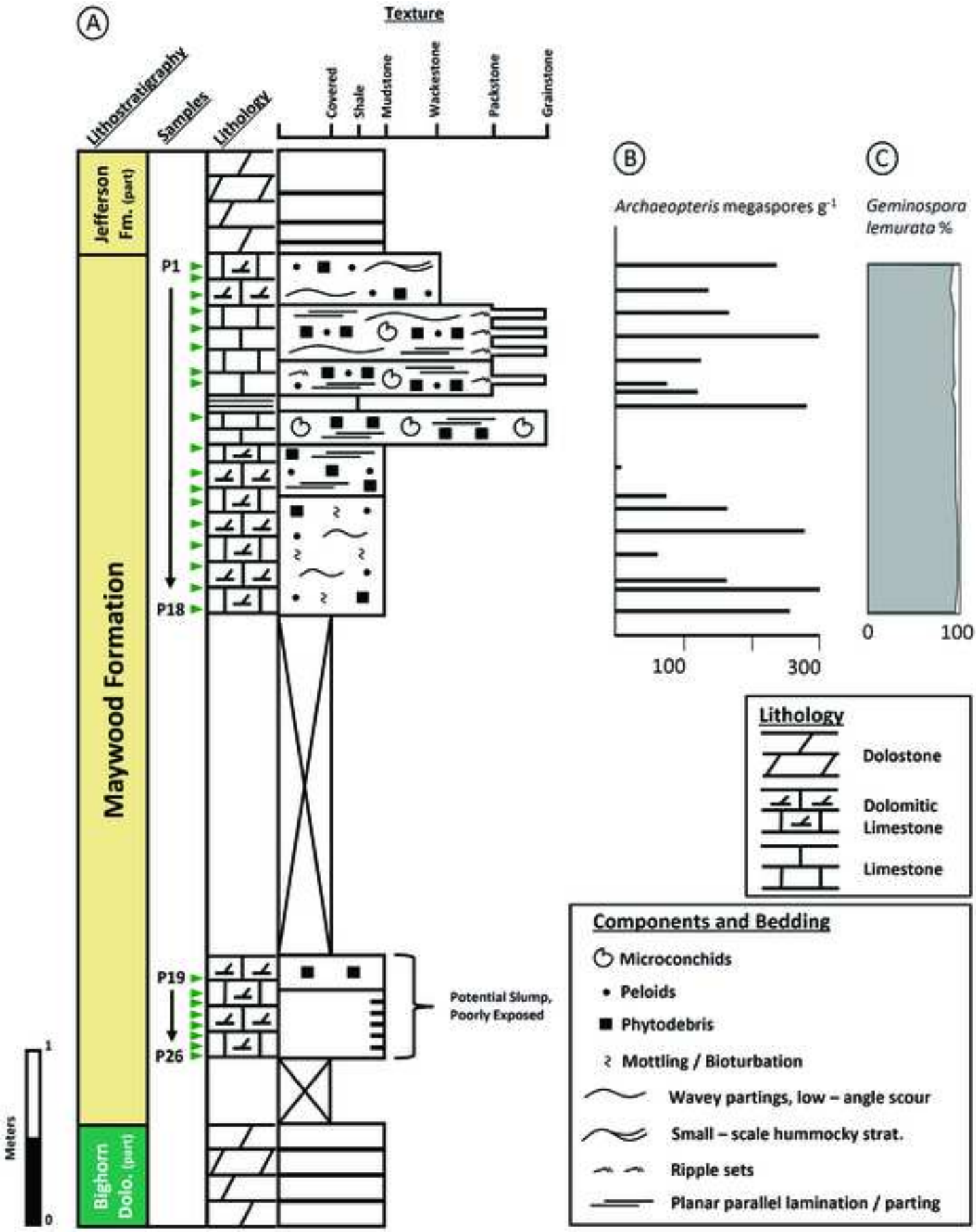

Figure 5

Click here to access/download;Figure;Figure5.tif

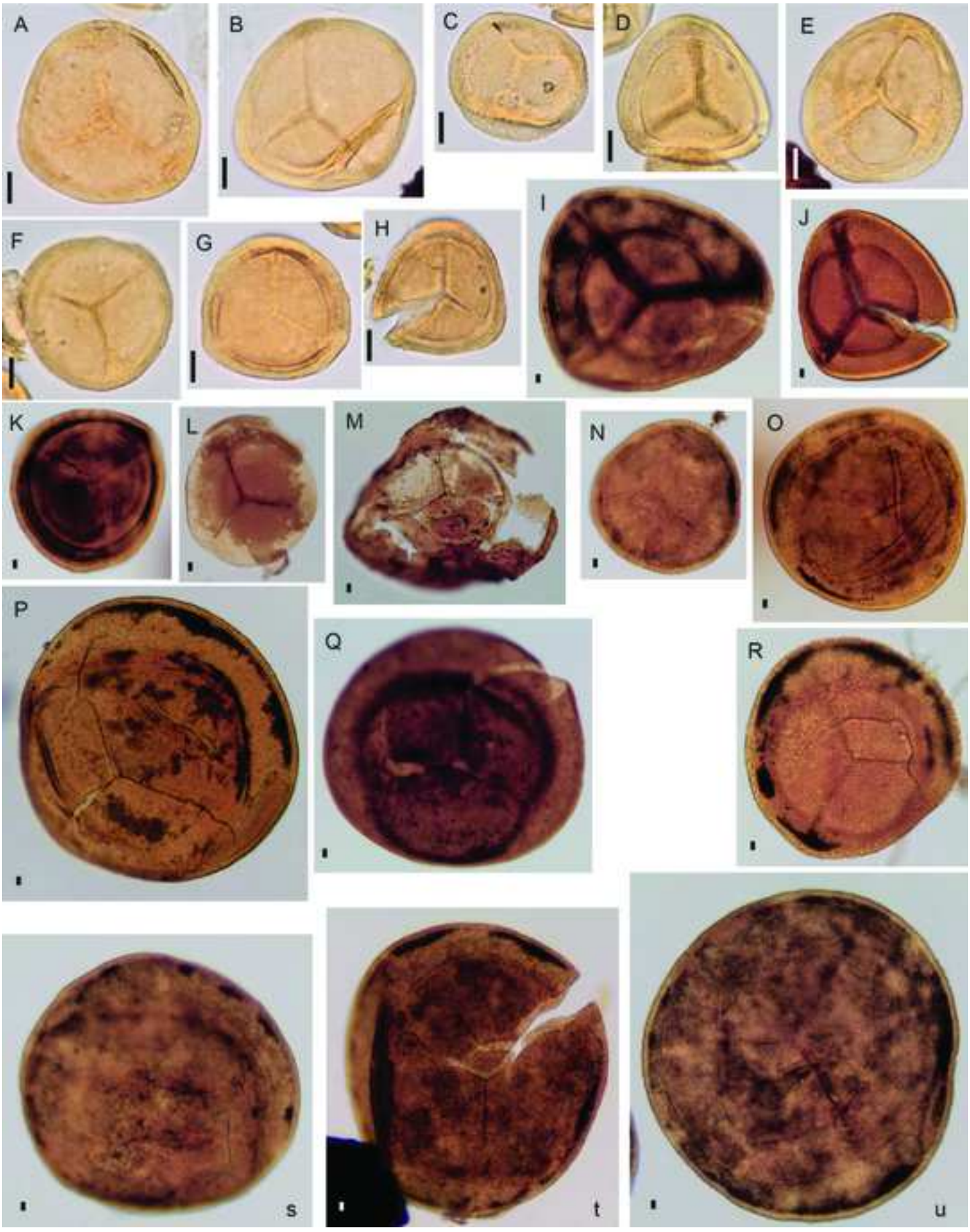

Figure 6

Click here to access/download;Figure;Figure6.tif

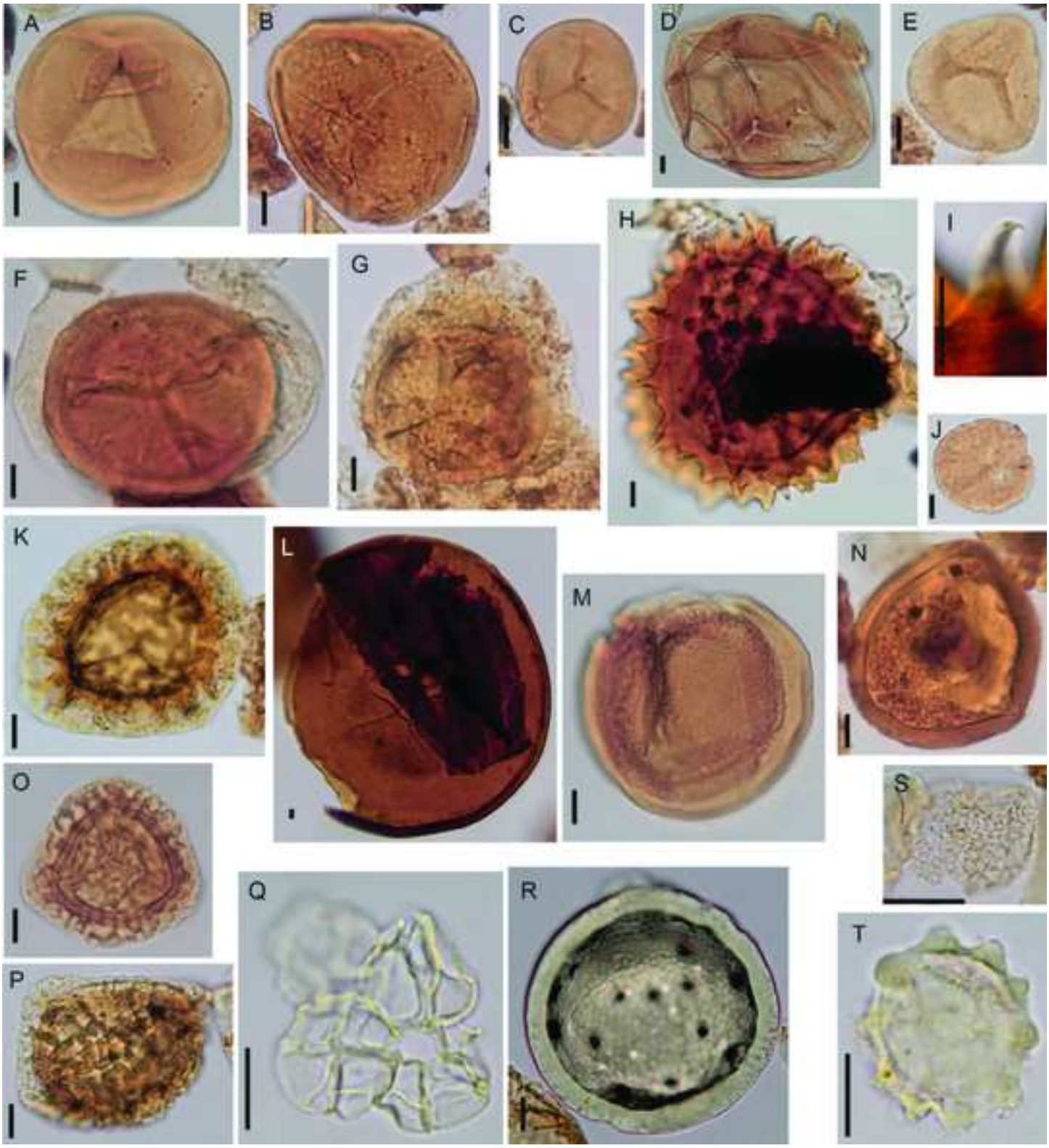

Figure 7



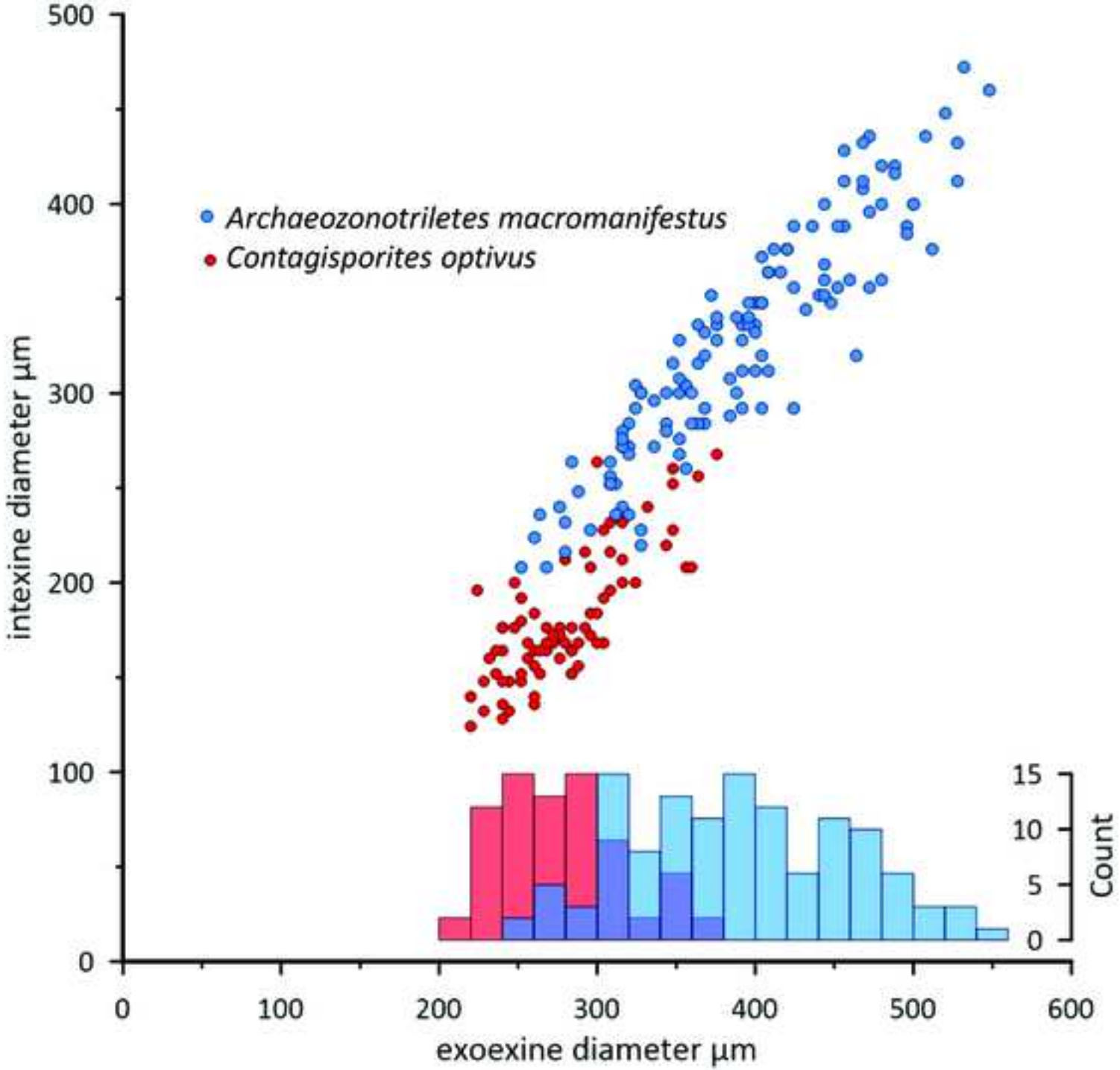

Figure 8

Click here to access/download;Figure;Figure8_tones.tif

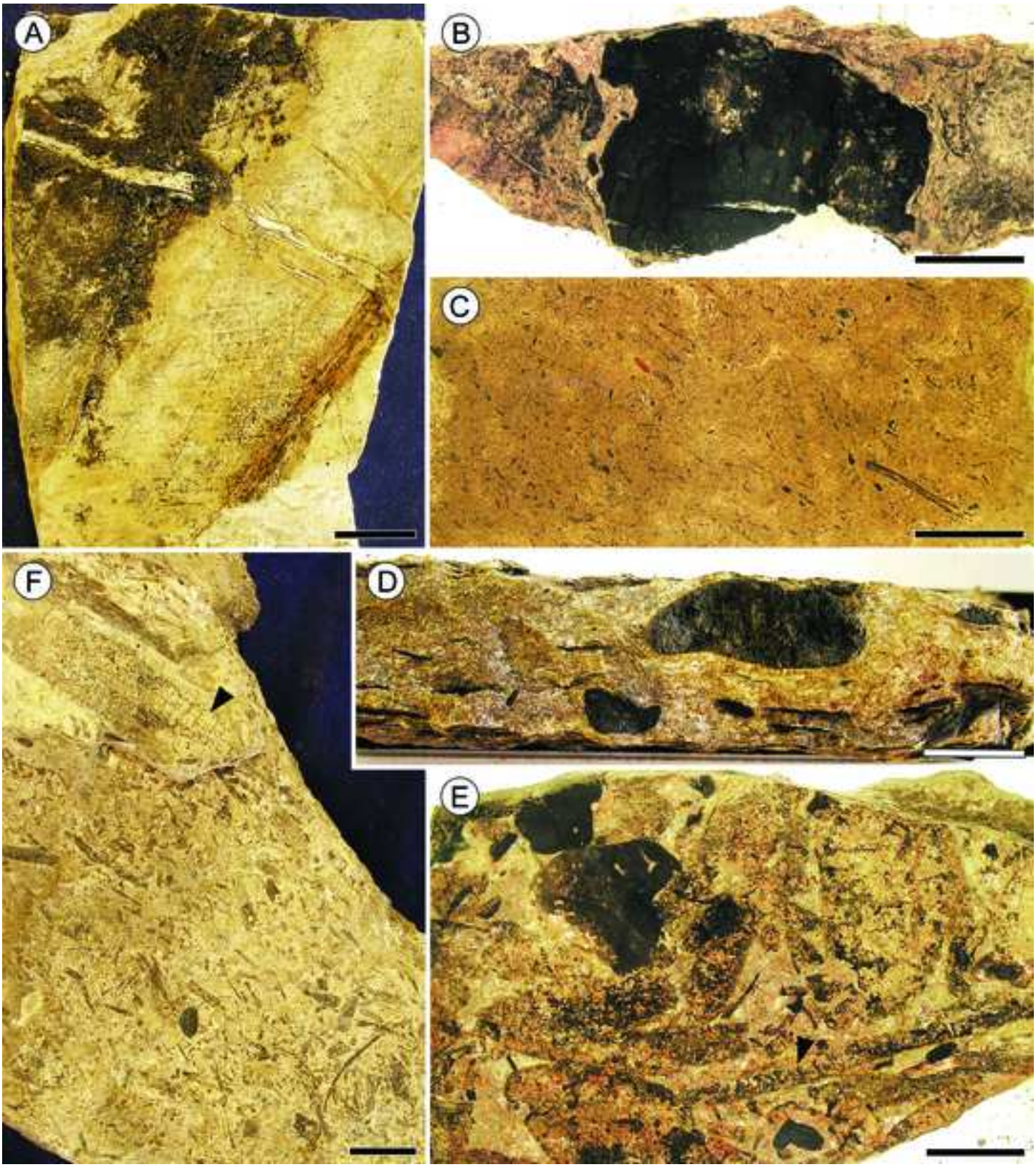

Figure 9

Click here to access/download;Figure;Figure9_tones.tif

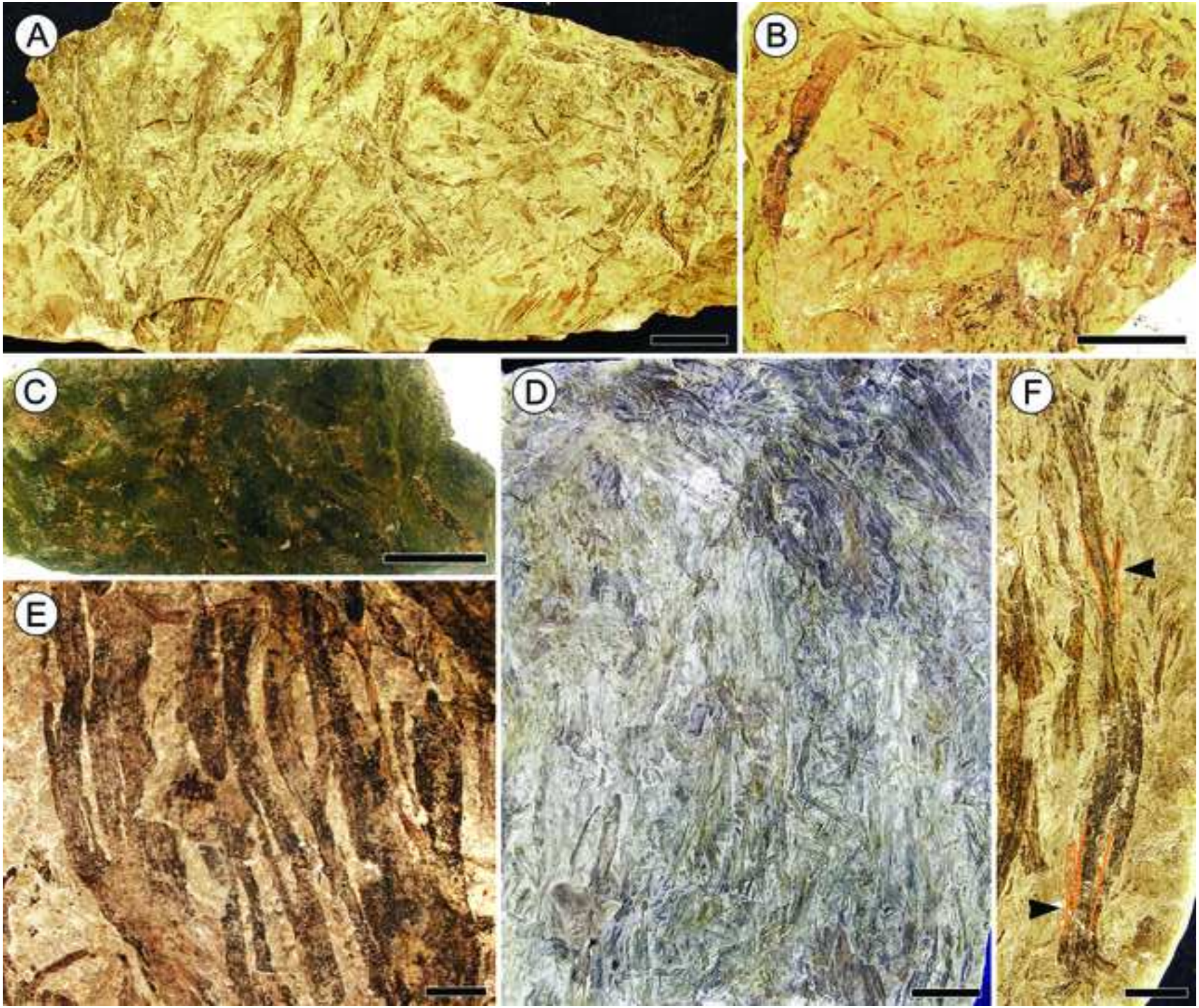

Figure 10

Click here to access/download;Figure;Figure10_tones.tif

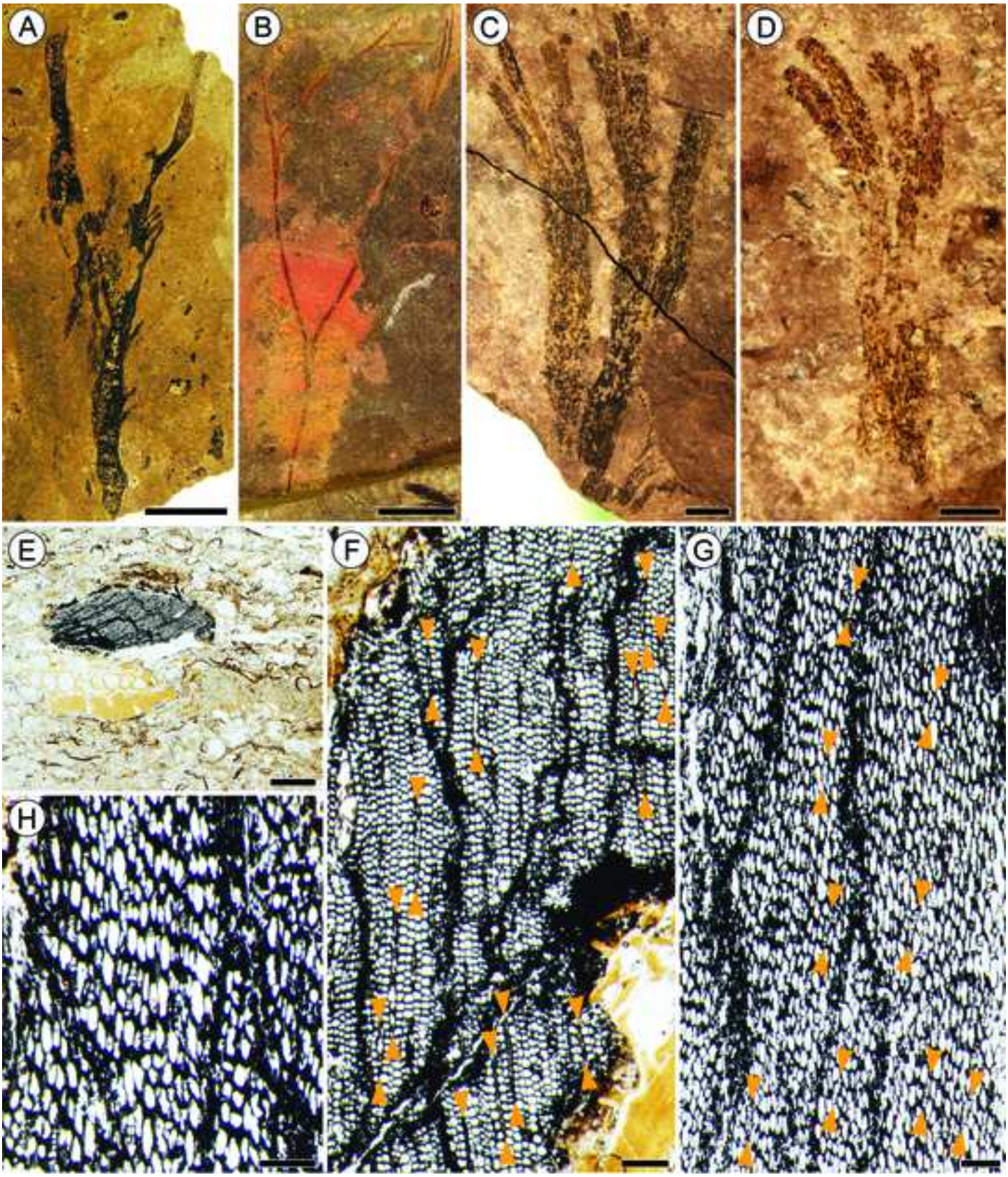

Figure 11

Click here to access/download;Figure;Figure11_tones.tif

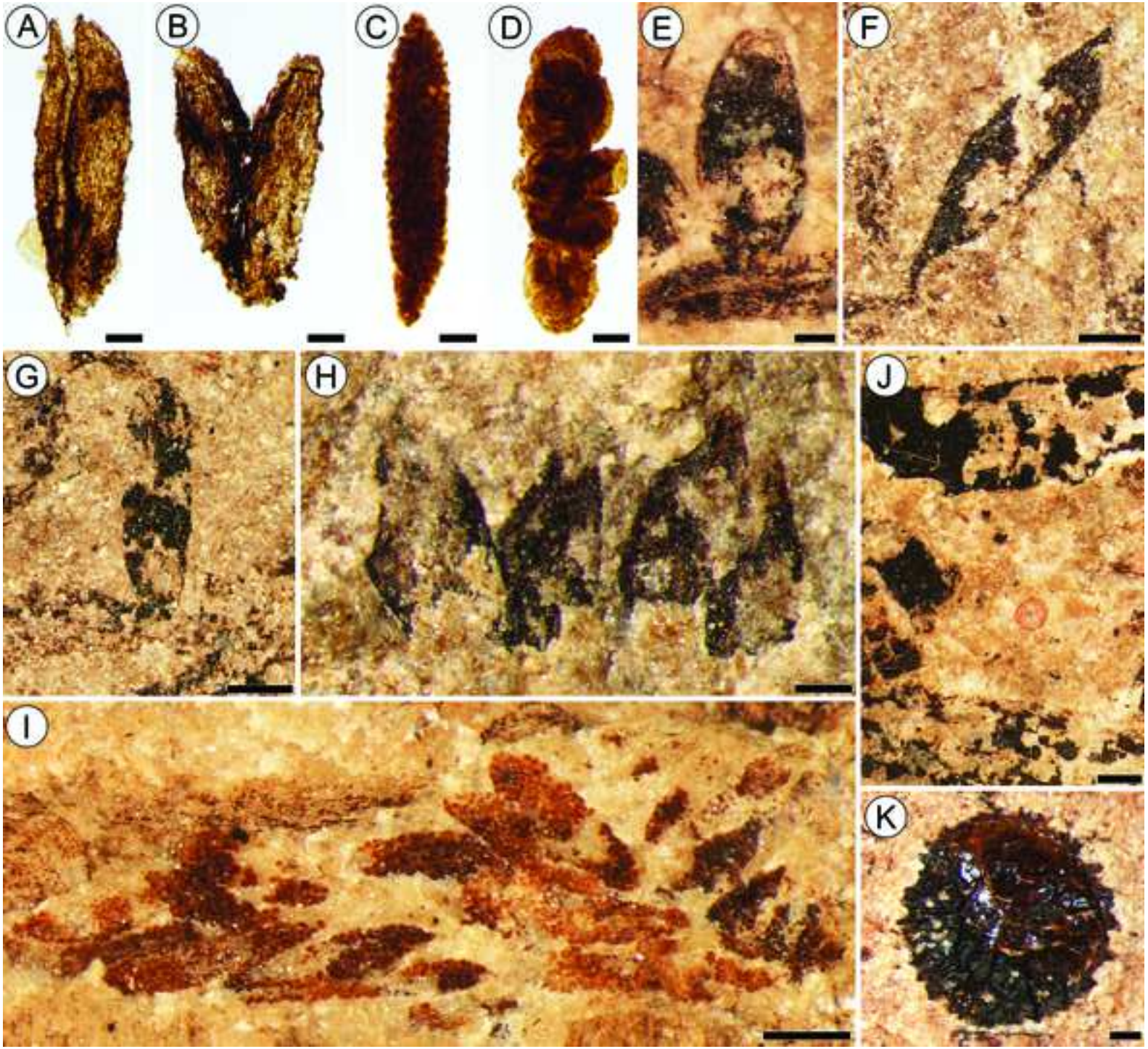

Figure 12

Click here to access/download;Figure;Figure12_tones.tif

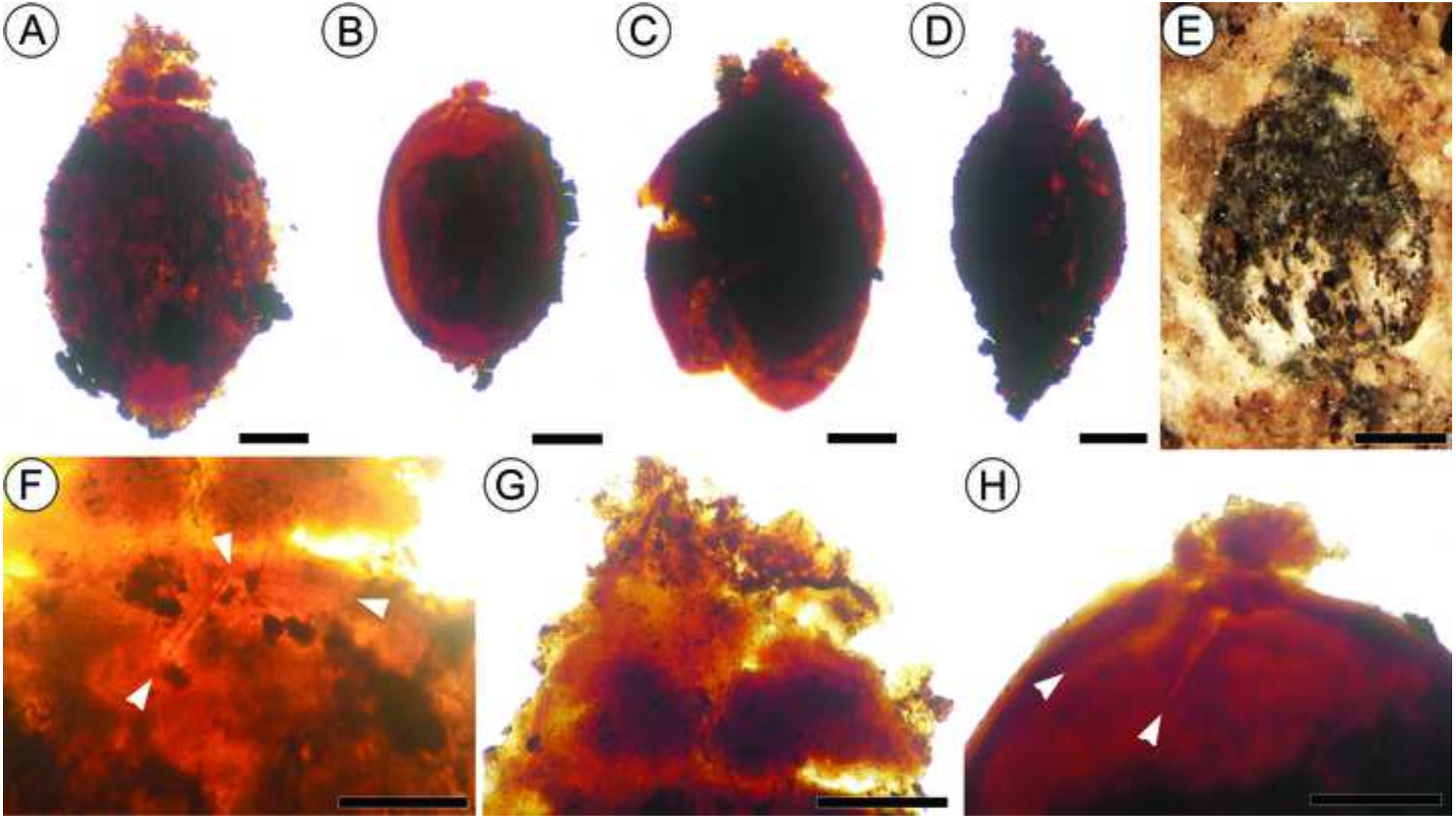

Figure 13

Click here to access/download;Figure;Figure13_tones.tif

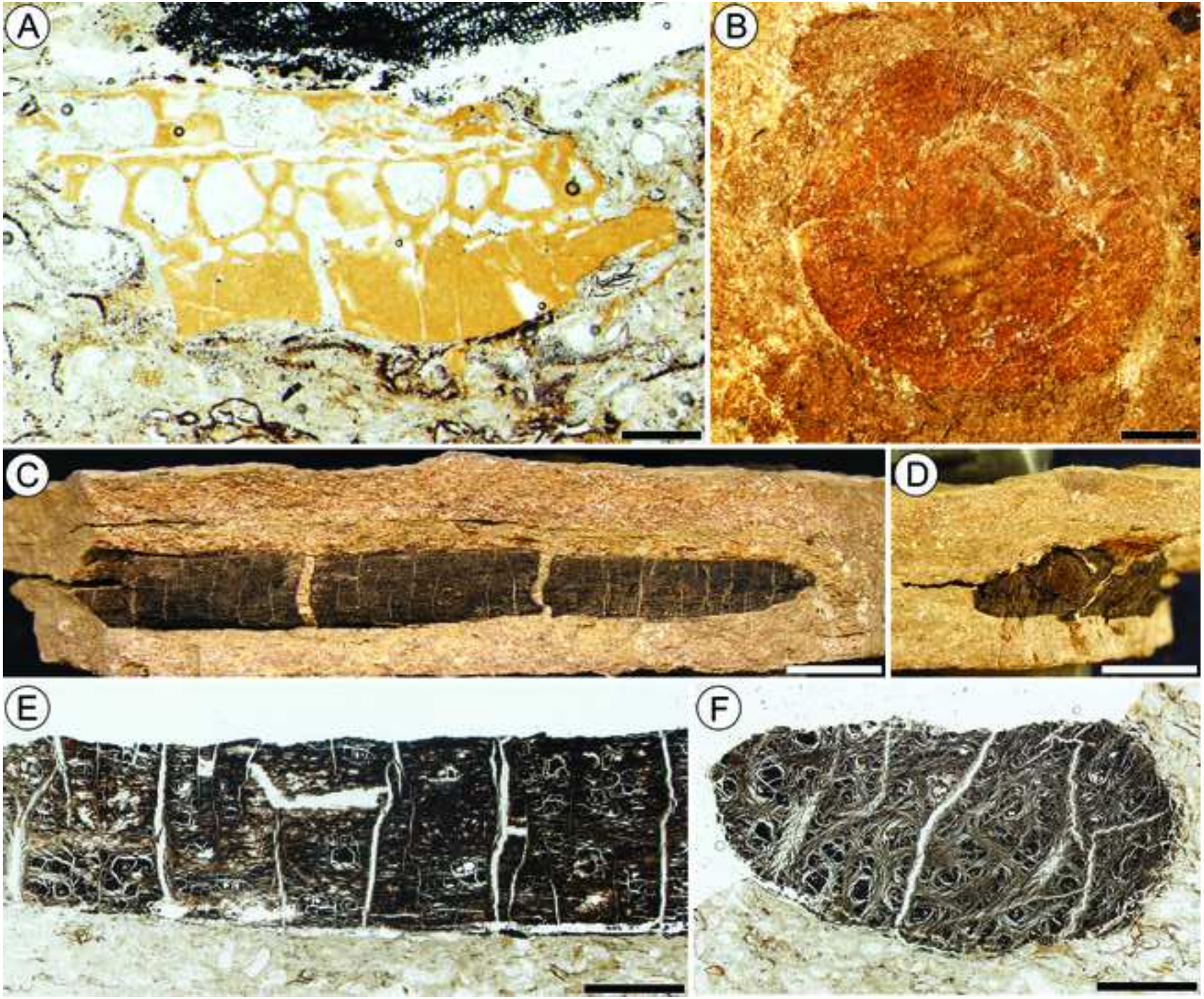

Figure 14

Click here to access/download;Figure;Figure14.tif

# THE ARCHAEOPTERID FORESTS OF WYOMING: FLORA AND DEPOSITIONAL ENVIRONMENT OF THE UPPER DEVONIAN (LOWER FRASNIAN) MAYWOOD FORMATION

John E.A. Marshall, Peter F. Holterhoff, Samar R. El-Abdallah, Kelly K.S. Matsunaga, Allison W. Bronson, Alexandru M.F. Tomescu

**Appendix 1** Supplemental figures

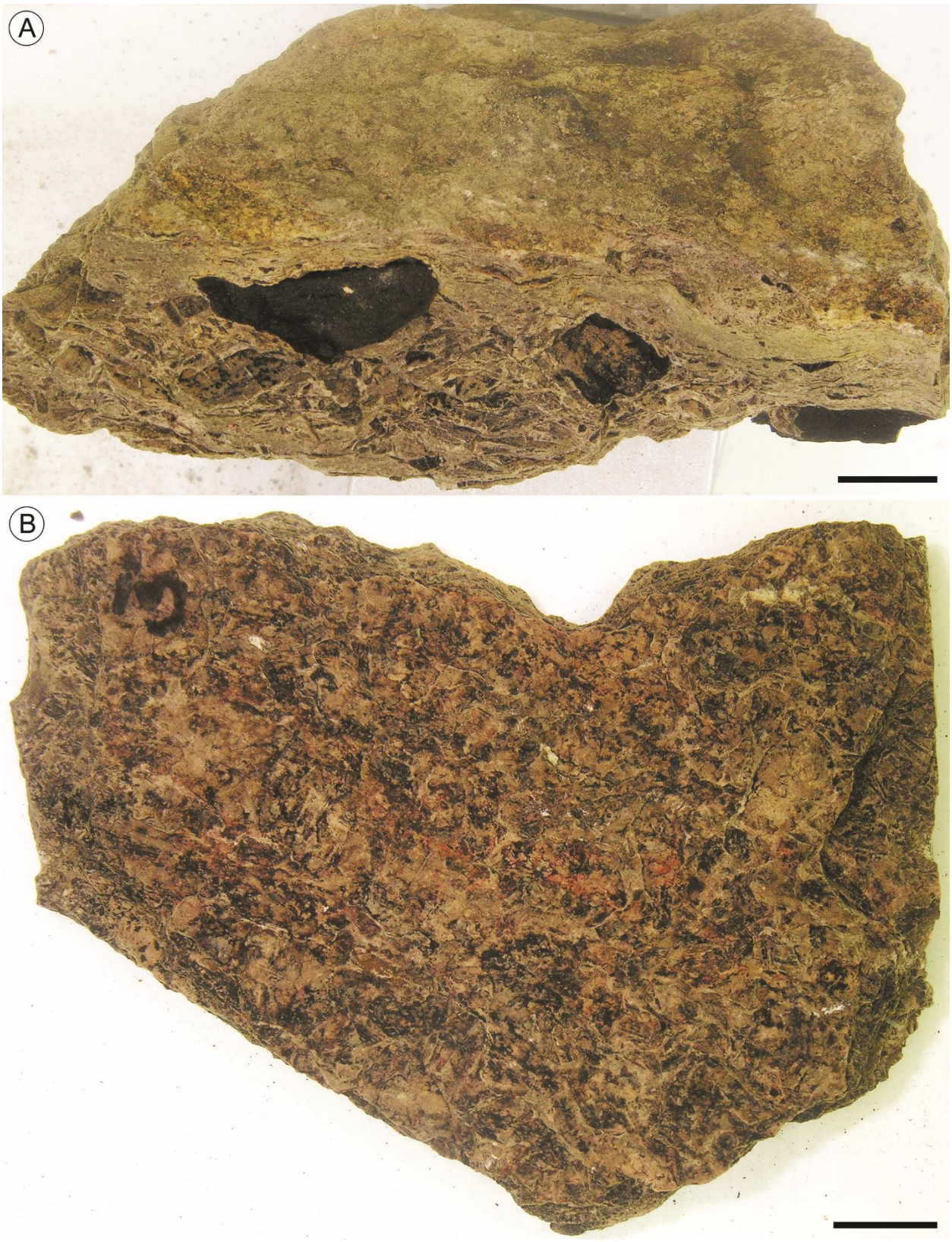
A
B

**Supplemental fig. 1** Macroflora of the Maywood Formation in Cottonwood Canyon (Wyoming); charcoalified material and adpressions. *A*, Oblique view of vertical plane of fracture in the layers; note rounded and angular wood charcoal fragments of different sizes, oriented with their long axes parallel to bedding planes; HPH711; scale 1 cm. B, Fragmented plant material exposed in large quantities on a bedding plane; HPH735; scale 1 cm.

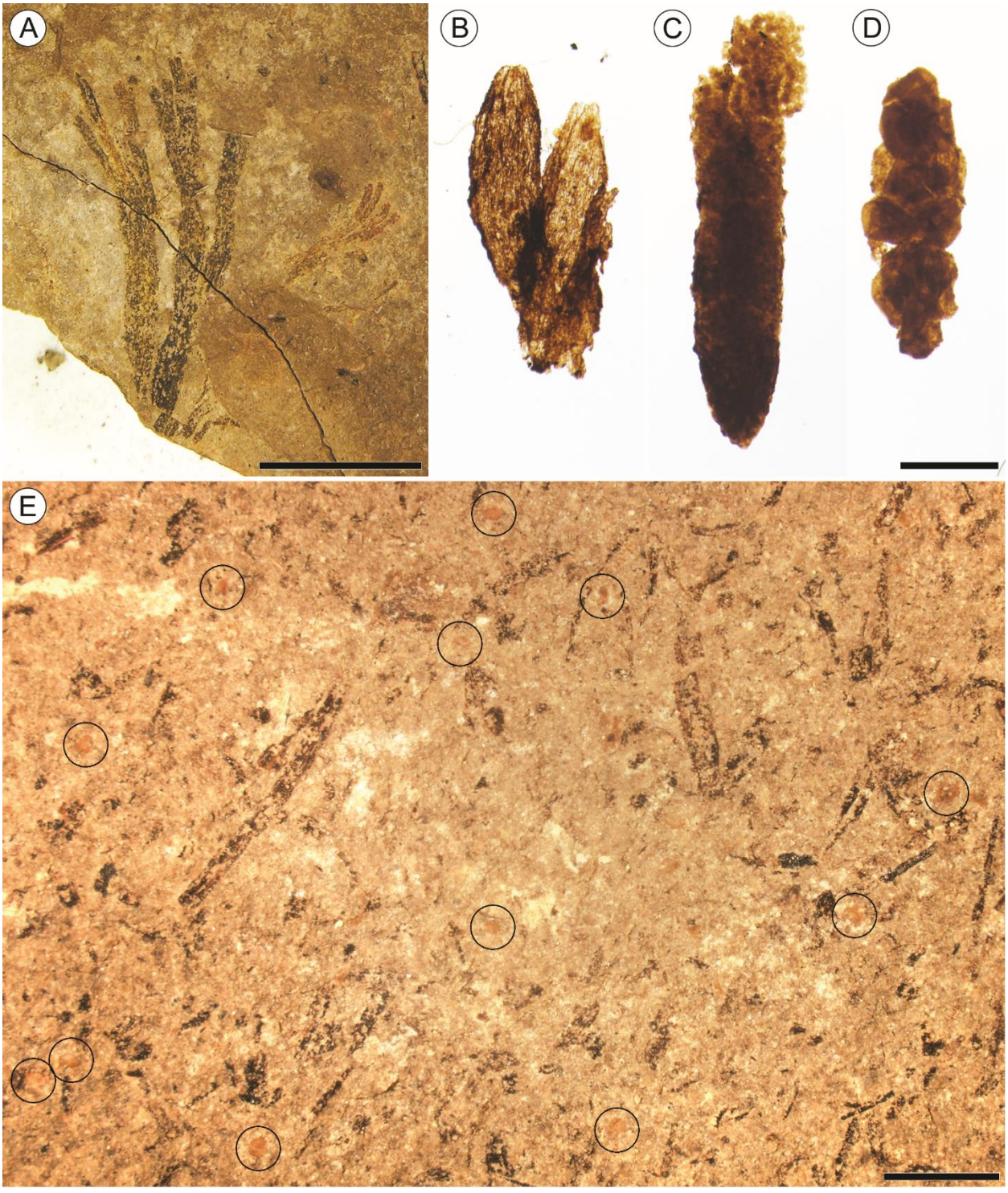
A
B
C
D
E

**Supplemental fig. 2** Flora of the Maywood Formation in Cottonwood Canyon (Wyoming). *A*, Fan-shaped leaves dissected into strap-shaped distal lobes with rounded margin; HPH721; scale 1 cm. *B*, Archaeopterid sporangia with fusiform shape retrieved from rock macerates; note epidermis with long narrow cells, dehiscence line that runs the entire length of the sporangium; HPH736. *C*, *D*, Clumps of archaeopterid spores (*C* – microspores; *D* – megaspores) retrieved from rock macerates, representing undissociated contents of sporangia; HPH737 (*C*); HPH738 (*D*); *B*, *C*, *D* scales 500 µm. *E*, Bedding plane with small evenly distributed charcoal and coalified plant fragments; note multiple megaspores (circled); HPH739; scale 2 mm.

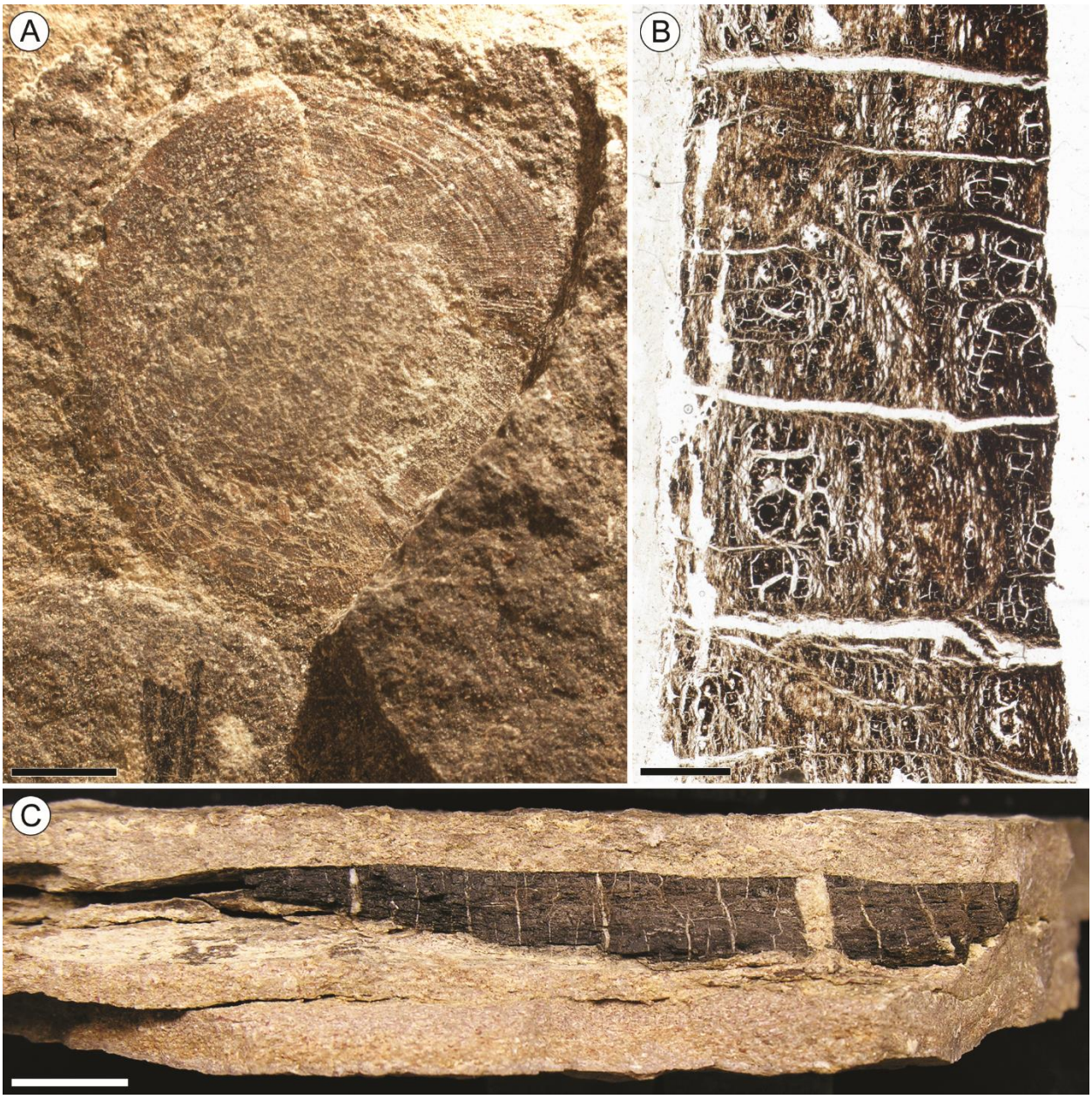
A
B
C

**Supplemental fig. 3** Animal fossils in the Maywood Formation at Cottonwood Canyon (Wyoming). *A*, Isolated sarcopterygian fish scale exposed on bedding plane; note round outline with fine anteroposteriorly oriented ridges on the posterior edge (bottom right) and low tubercles in the anterior area (top left and toward center of scale), similar to tetrapodomorph scales; HPH734; scale 2 mm. *B*, Longitudinal section of object interpreted as coprolite; note amorphous material that forms "swirly" texture around "nests" of angular fragments, and network of fine diagenetic mineral precipitation veins; HPH722 slide 7; scale 1 mm. *C*, Elongated dark brown object deposited parallel with the bedding planes, interpreted as a coprolite; note orthogonal network of fine diagenetic mineral precipitation veins crossing the object; HPH722; scale 1 cm.